U.S. Department
of Transportation
**Federal Railroad
Administration**

# Tank Car Damage Assessment Procedure Study

Office of Research and
Development
Washington, D.C. 20590

William P. Wright

Department of Army
U.S. Armament, Munitions and Chemical Command
Ballistic Research Laboratory
Aberdeen Proving Ground, Maryland 21005

DOT/FRA/ORD-84/04

May 1984
Final Report

NOTICE

This document is disseminated under the sponsorship of the Department of Transportation in the interest of information exchange. The United States Government assumes no liability for the contents or use thereof.

**Technical Report Documentation Page**

| 1. Report No. | 2. Government Accession No. | 3. Recipient's Catalog No. |
|---|---|---|
| FRA/ORD-84/04 | | |

| 4. Title and Subtitle | 5. Report Date |
|---|---|
| TANK CAR DAMAGE ASSESSMENT PROCEDURE STUDY | May 1984 |
| | 6. Performing Organization Code |
| | 8. Performing Organization Report No. |
| 7. Author(s) William P. Wright | |
| 9. Performing Organization Name and Address<br>USA AMCCOM, ARDC<br>ATTN: DRXMC BLT(A)<br>Ballistic Research Laboratory<br>Aberdeen Proving Ground, MD 21005 | 10. Work Unit No. (TRAIS) |
| | 11. Contract or Grant No.<br>A.N. DTFR53-82-X-00275 |
| 12. Sponsoring Agency Name and Address<br>Department of Transportation<br>Federal Railroad Administration<br>Office of Research and Development<br>Washington, DC 20590 | 13. Type of Report and Period Covered<br>Final<br>October 82 to February 84 |
| | 14. Sponsoring Agency Code |

15. Supplementary Notes

This study was funded by the Federal Railroad Administration of the Department of Transportation.

16. Abstract

The study concerns the rupture of damaged tank cars which have been involved in railroad accidents. In this regard, a series of impact tests using the FRA/BRL Drop Hammer Facility was performed. The tests consisted of the creation of controlled damage to flat steel plates which had properties exceeding the minimum ASTM standards required for steel used in the construction of tank cars (ASTM A-515, Grade 70 steel). The plates responded in the form of dents which reflected the shapes and sizes of tups which were driven onto the plates and the sizes of dies on which the plates were placed. As expected, the shapes of the dents were similar to the shapes of the tups and as the dies were changed to larger diameters, the amount of bending increased. A total of 70 tests were conducted with various hammer heights, tup shapes and sizes, and die diameters. The maximum dent depth as a function of impacting kinetic energy was shown to be a scaling function. Several of the plates were analyzed using NDE techniques (ultrasonics and dye penetrant) and fracture mechanical procedures. Several important correlations were discovered between the dent characteristics and levels of flaw damage found in the material. The results were encouraging and a series of tasks are identified as the best approach for continuing on toward a final solution.

| 17. Key Words | 18. Distribution Statement |
|---|---|
| Railroad Tank Cars<br>Safety<br>Nondestructive Evaluation<br>Fracture Mechanics | Document is available to the U.S. public through the National Technical Information Service, Springfield, Virginia 22161 |

| 19. Security Classif. (of this report) | 20. Security Classif. (of this page) | 21. No. of Pages | 22. Price |
|---|---|---|---|
| Unclassified | Unclassified | 24 | |

Form DOT F 1700.7 (8-72) Reproduction of completed page authorized

# METRIC CONVERSION FACTORS

## Approximate Conversions to Metric Measures

| Symbol | When You Know | Multiply by | To Find | Symbol |
|---|---|---|---|---|
| | | **LENGTH** | | |
| in | inches | *2.5 | centimeters | cm |
| ft | feet | 30 | centimeters | cm |
| yd | yards | 0.9 | meters | m |
| mi | miles | 1.6 | kilometers | km |
| | | **AREA** | | |
| $in^2$ | square inches | 6.5 | square centimeters | $cm^2$ |
| $ft^2$ | square feet | 0.09 | square meters | $m^2$ |
| $yd^2$ | square yards | 0.8 | square meters | $m^2$ |
| $mi^2$ | square miles | 2.6 | square kilometers | $km^2$ |
| | acres | 0.4 | hectares | ha |
| | | **MASS (weight)** | | |
| oz | ounces | 28 | grams | g |
| lb | pounds | 0.45 | kilograms | kg |
| | short tons (2000 lb) | 0.9 | tonnes | t |
| | | **VOLUME** | | |
| tsp | teaspoons | 5 | milliliters | ml |
| Tbsp | tablespoons | 15 | milliliters | ml |
| fl oz | fluid ounces | 30 | milliliters | ml |
| c | cups | 0.24 | liters | l |
| pt | pints | 0.47 | liters | l |
| qt | quarts | 0.95 | liters | l |
| gal | gallons | 3.8 | liters | l |
| $ft^3$ | cubic feet | 0.03 | cubic meters | $m^3$ |
| $yd^3$ | cubic yards | 0.76 | cubic meters | $m^3$ |
| | | **TEMPERATURE (exact)** | | |
| °F | Fahrenheit temperature | 5/9 (after subtracting 32) | Celsius temperature | °C |

*1 in. = 2.54 cm (exactly). For other exact conversions and more detail tables see NBS Misc. Publ. 286, Units of Weight and Measures. Price $2.25 SD Catalog No. C13 10 286.

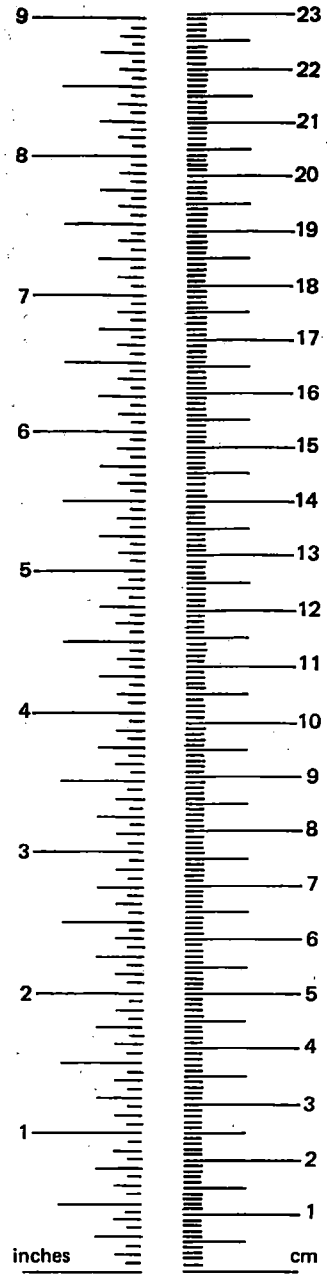


## Approximate Conversions from Metric Measures

| Symbol | When You Know | Multiply by | To Find | Symbol |
|---|---|---|---|---|
| | | **LENGTH** | | |
| mm | millimeters | 0.04 | inches | in |
| cm | centimeters | 0.4 | inches | in |
| m | meters | 3.3 | feet | ft |
| m | meters | 1.1 | yards | yd |
| km | kilometers | 0.6 | miles | mi |
| | | **AREA** | | |
| $cm^2$ | square centimeters | 0.16 | square inches | $in^2$ |
| $m^2$ | square meters | 1.2 | square yards | $yd^2$ |
| $km^2$ | square kilometers | 0.4 | square miles | $mi^2$ |
| ha | hectares (10,000 $m^2$) | 2.5 | acres | |
| | | **MASS (weight)** | | |
| g | grams | 0.035 | ounces | oz |
| kg | kilograms | 2.2 | pounds | lb |
| t | tonnes (1000 kg) | 1.1 | short tons | |
| | | **VOLUME** | | |
| ml | milliliters | 0.03 | fluid ounces | fl oz |
| l | liters | 2.1 | pints | pt |
| l | liters | 1.06 | quarts | qt |
| l | liters | 0.26 | gallons | gal |
| $m^3$ | cubic meters | 36 | cubic feet | $ft^3$ |
| $m^3$ | cubic meters | 1.3 | cubic yards | $yd^3$ |
| | | **TEMPERATURE (exact)** | | |
| °C | Celsius temperature | 9/5 (then add 32) | Fahrenheit temperature | °F |

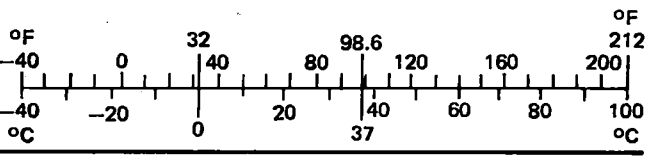

## EXECUTIVE SUMMARY

The Tank Car Damage Assessment Project as discussed in this report was defined by the Federal Railroad Administratin (FRA) of the Department of Transportation (DOT). The basis for interest in this work was that due to tank car ruptures following the initial neutralization of hazards, a minimum of 24 fatalities and 118 injuries had occurred prior to this work. The Ballistic Research Laboratory (BRL) was funded by the FRA to execute a research program for the purpose of developing a feasible procedure for reducing the potential for casualties under these circumstances. A main feature of the plan was to be the use of advanced technology in nondestructive evaluation (NDE) techniques and computer equipment.

The BRL initially performed a literature search and devised a basic approach for attacking the problem. As the work proceeded, it became clear that experts in the field of NDE applications would be required and that the procurement of NDE equipment in certain categories would be prohibitive from a cost point of view. Consequently, the Materiel Testing Directorate (MTD), located at Aberdeen Proving Ground, was asked to apply NDE techniques available to them to several damaged steel plates and a damaged 1/5 scale tank car model. At the same time, the Idaho National Engineering Laboratory (INEL), located at Idaho Falls, Idaho, was requested to perform a similar task on a number of steel plates. It was found that the NDE techniques which have the greatest potential for use in this problem are ultrasonics, acoustic emission, and infra-red detection devices.

It was concluded that the tasks needed to resolve the problem are as follows: (1) A data base consisting of categories of flaws in tank car type materials needs to be created. (2) Correlations between flaw characteristics and metalurgical (fracture mechanics) parameters and further correlations with levels of applied stress leading to failure should be discovered. (3) An elastic-plastic stress analysis should be performed of typically damaged tank cars to determine the levels of stress existing during tank car wreck clearing operations. (4) And finally, model tank cars need to be tested to verify the technology developed, and, after appropriate adjustments, a full scale tank car should be tested for final verification.

## TABLE OF CONTENTS



## LIST OF FIGURES

LIST OF TABLES



LIST OF SYMBOLS

Symbols

AAR - Association of American Railroads
AE - Acoustic Emission
ASTM - American Society for Testing and Materials
a - Crack Depth
$^{o}C$ - Degree Centigrade
BRL - Ballistic Research Laboratory
cc - Cubic Centimeter
CGA - Compressed Gas Association
cm - Centimeter
2c - Crack Length
DOT - Department of Transportation
DM - Dial Micrometer
DH - Drop Hammer
DD - Depth of Dent
$D_D$ - Die Diameter
D - Tup Diameter
d - Thickness of Plate
E - Plate Density Times Tup Velocity Squared
$^{o}F$ - Degree Fahrenheit
FRA - Federal Railroad Administration
gm - Gram
HH - Hammer Height
INEL - Idaho National Engineering Laboratory
ID - Identification Number
in. - Inch (Inches)
Kgs - Kilograms
$K_{Ic}$ - Plane Strain Fracture Toughness
$K_I$ - Applied Stress Intensity Factor
Ksi - 1000 psi
LPG - Liquid Petroleum Gas
LEFM - Linear Elastic Fracture Mechanics
MHz - Megahertz
Mpa - Megapascal
psi - Pounds/square inch
m - Meter
NDE - Nondestructive Evaluation
NDT - Nondestructive Testing
NTSB - National Transportation Safety Board
S - Ultimate Strength of Plate Material
sec - Second
$T_{LF}$ - 5.5 Inch Diameter Flat Tup
$T_{LH}$ - 5.5 Inch Diameter Hemispherical Tup
$T_{MH}$ - 3.75 Inch Diameter Hemispherical Tup
$T_{SH}$ - 2.0 Inch Diameter Hemispherical Tup
$^{o}K$ - Degree Kelvin

## INTRODUCTION

The Ballistic Research Laboratory (BRL) was under contract to the Federal Railroad Administration (FRA) of the Department of Transportation (DOT) to investigate the feasibility of utilizing nondestructive evaluation (NDE) techniques for the purpose of assessing the damage of derailed tank cars containing hazardous materials. For example, a damaged tank car carrying liquid petroleum gas (LPG) under pressure constitutes an extreme hazard such that the tank car should be approached with great caution. In this area of study, the goal is to develop adequate procedures for making accurate evaluations before and during the moving and/or unloading of a damaged tank car. These procedures will make use of NDE techniques in combination with an extensive data base which describes various categories of flaws in tank car type materials. A secondary and much less difficult task is to determine the best NDE techniques for the inspection of tank cars during manufacturing processes and shop repairs.

Historical data supporting the decision to engage in these studies include the fact that 24 fatalities and 118 injuries have been sustained in recent years due to tank car ruptures during wreck-clearing operations. The worse case occurred following a 23 car derailment at Waverly, Tennessee on February 24, 1978 (Ref 1). In that case, a damaged tank car containing LPG ruptured two days after a derailment during preparations for having its lading transferred. The lading was released and the ensuing fire killed 16 persons and injured 43 others. Another incident occurred on April 18, 1979 at Crestview, Florida, where several wreck-clearing personnel were exposed to anhydrous ammonia from a tank car which unexpectedly ruptured (Ref. 2). These incidents show that wreck-clearing crews, emergency response teams, and the public are in danger even after the initial hazards in a derailment involving hazardous materials have been neutralized.

The difficulty in assessing a wrecked tank car was dramatized in a study conducted by the National Transportation Safety Board (NTSB) (Ref. 3). That study had the following three objectives - (1) to identify the hazards associated with a degradation in the ability of damaged tank cars to contain their lading; (2) to determine the ability of experts to estimate this reduced capability; and (3) to examine the feasibility of developing practical guidelines to help determine how damaged tank cars loaded with a hazardous material should be handled. Cooperating with the NTSB as parties to this special investigation were the FRA, the Association of American Railroads (AAR), the Compressed Gas Association (CGA), Hulcher Emergency Services, and the General American Transportation Corporation. In this study a damaged tank car which had been relieved of its lading was examined and evaluated by persons who were considered experts. The tank car was subsequently hydrostatically pressurized to failure. The results of this exercise caused the NTSB to conclude the following:

"The failure pressures of the tank and the potential failure area were not accurately predicted by the investigation group. The tank actually ruptured at a pressure 40 percent below the minimum estimated failure pressure, and the failure originated at an unexpected location. It should be pointed out, however, that the estimates were made using only visual examination. Although magna flux and dye penetrant would normally be available in the field, they are not always used. Of course, in the case of a loaded car, no inside testing could be done. The fact that experts had difficulty estimating failure modes and pressures, demonstrates that adequate safety guidelines do not currently exist. The accident history of tank car ruptures at accident sites establishes a need for such guidelines."

The FRA provided the BRL initial guidelines for setting up a study program. It was pointed out that the damaged tank car in an accident would require the use of nondestructive evaluation (NDE)* techniques and that these would have to be investigated to determine the most useful ones for this application. Once identified, the required equipment associated with each NDE technique were to be listed. Model tank cars were to be procured which could be used in a test program where the various NDE techniques were to be applied. These techniques were then to be evaluated in terms of effectiveness in yielding data that could be used to assess the tank car damage. Once the evaluation of the damage becomes completed, suitable destructive testing (metallurgical evaluation and fracture mechanics) were to be conducted for verification. Based on these studies, a complete set of wreck-clearing procedures were to be developed and a plan devised for full scale testing.

The BRL conceived several concepts for addressing the basic problems listed by the FRA. In addition to clearing wrecked tank cars, the FRA wanted evaluation techniques developed for tank car manufacturing and tank car repairs. It was decided that the problems associated with the

[1] *"Railroad Accident Report-Derailment of Louisville and Nashville Railroad Company's Train No. 584 and Subsequent Rupture of Tank Car Containing Liquefied Petroleum Gas, Waverly, Tennessee, February 22, 1978", NTSB-RAR-79-1, U.S. National Transportation Safety Board, Washington, D.C. 20594, 8 February, 1979.*

[2] *"Railroad Accident Report-Louisville and Nashville Railroad Company Freight Train Derailment and Puncture of Hazardous Materials Tank Cars, Crestview, Florida, April 8, 1979", NTSB-RAR-79-11, U.S. National Transportation Safety Board, Washington, D.C. 20594, September 1979.*

[3] *"SPECIAL INVESTIGATION REPORT - Tank Car Structural Integrity After Derailment", NTSB-SIR-80-1, U.S. National Transportation Safety Board, Washington, D.C. 20594, October 16, 1980*

**Nondestructive testing (NDT) is a term synonymous with nondestructive evaluation (NDE), but the latter term appears more appropriate and is used throughout the text.*

clearing of an accident site are the most difficult to resolve and that information gained in determining appropriate procedures for that kind of operation would automatically present methods for manufacturing and repairs. The second is to separate the clearing of tank car procedure into three phases. The first is to develop methods for evaluating the tank car from a safe distance to ascertain if the car can be safely approached. The second is to develop methods for making an accurate evaluation as a result of being able to touch the tank car and apply nondestructive evaluation (NDE) techniques. (Under some circumstances it may be possible and desirable to attach the NDE devices, retreat a safe distance, and then execute a remote evaluation.) The third is to develop techniques for monitoring the tank car's condition as the wreck-clearing operation proceeds. The latter is necessary to serve as a warning mechanism to the wreck-clearing crew that a deterioration of the situation has occurred and to give the crew time to evacuate.

## NDE TECHNIQUES REVIEW

Ultrasonic sound waves is one of the most important NDE techniques available. (Ref. 4 & 5). The technique consist of the placement of a transducer next to the surface of a specimen to be inspected. The transducer generates a ultrasonic sound wave which travels through the specimen in a particular incident angle and direction. In the event no flaw or other discontinuity is present, the echo of the sound wave is detected by the transducer with no variation in the spectrum from the known form. In the event a flaw is present, the ultrasonic system can locate and characterize the flaw in terms of size, shape, orientation, and composition by studying the variation in the echo signal. In the event a data base describing categories of flaws and their characteristics is available in a computer bank, a specific echo signal can be evaluated automatically by having a computer make the appropriate comparisons and a read out of the result. With the advent of relatively cheap computer technology, the value of ultrasonics as an NDE technique increased because the technique is amenable to automation. The primary disadvantage of ultrasonics with regard to the tank car damage assessment problem is that the transducer must be touching the surface of the tank car and therfore any coating such as a thermal insulation must be removed.

Ultrasonic techniques for the detection of flaws are generally based on measurements of attenuation or reflection of longitudinal or shear waves directed into the specimen, or on similar measurements with surface waves. One of the most important applications of ultrasonic NDE technology is the detection of fatigue cracks or other near-surface defects in metallic specimens. Surface waves, i.e. Rayleigh waves in thick specimens or Lamb (flexural) waves in thin sheets, are particularly useful for this purpose because they naturally follow the contours of the piece being inspected. In the case of attenuation, the presence of defects is detected as a change in amplitude of the echo pattern. For reflection experiments, the pulse-echo type involves the detection of ultrasonic waves scattered by flaws. From this information flaw location, size, shape and orientation can be determined.

Ultrasonic methods can be used to evaluate the metallurgical state of a specimen by the measurement of attenuation and/or phase velocity. For example, ultrasonic attenuation data can often be correlated with grain size of the precipitate or second phase particles in a metal matrix. The usefulness of sound velocity data derives from the fact that the sound velocity depends on the values of the elastic constants and these, in turn, depend on residual stress, grain orientation, density, and temperature.

As technology develops, systems tend to increase in complexity and degree of automation. Ultrasonic NDE technology has followed this trend. For example, most early ultrasonic NDE systems comprised a "home-made" or commercial pulser-receiver-display unit and a hand-held transducer which was manually scanned over the part to be inspected. Now, with recent rapid decreases in cost, size, and power requirements of general-purpose digital computers, highly automated, computer-based systems are appearing in the field of ultrasonic NDE. Although some automated systems are used in the laboratory for conducting experiments in ultrasonic inspection, many systems are working on the production line yielding high volume, high-quality inspection of basic material forms and fabricated structures.

Another NDE technique which depends on sound waves is referred to as acoustic emission (AE). The essence of this technique is that a transducer is used to detect sound generated by the growth of cracks in the specimen being tested. Those materials which generate the highest levels of acoustic signals are metallic brittle materials. However, even the relatively soft metals of which tank cars are made generate AE signals and these can be detected after other unwanted signals have been filtered out. The location of the flaw can be detected by using three transducers and a triangulation procedure. Since the flaw itself must generate the noise as it increases in size, the specimen must be under stress as the inspection is being made. For that reason, it is anticipated that AE will be an important mechanism for monitoring the tank car as it is being moved or the lading being unloaded. Such a monitoring system will also be important for use during the period over which a damaged tank car is waiting to be moved because of possible internal pressure build-up in the event the ambient temperature increases. AE devices should also be useful for detecting leaks since such leaks generate distinct sound waves. As with ultrasonics, AE is also amendable to computer techniques and automation. Consequently, AE will be studied as a serious candidate

[4] *Beissner, R.E., "Electromagnetic-Acoustic Transducers, A Survey of the State-Of-The-Art", Southwest Research Institute, San Antonio, Texas, NTIAC-76-1, January 1976.*

[5] *Silvus, Jr., H.S., "Advanced Ultrasonic Testing Systems, A State-Of-The-Art Survey", Southwest Research Institute, San Antonio, Texas, NTIAC-77-1, September 1976*

for application to the tank car damage assessment problem.

An NDE technique which has wide application is referred to as the Magnetic Leakage Field Method (Ref. 6). This method is based on the fact that a near surface discontinuity in the geometry or magnetic properties of a magnetized body produces a localized perturbation in the magnetic field just outside the surface of the body. Thus, in principal, the presence of a crack, nonmagnetic inclusion, or any other localized anomaly in magnetic properties can be detected by searching the surface of a specimen for localized fluctuations in the magnetic field. One of the methods of observing the variation in the magnetic field is the use of a fine powder of iron particles which is applied to the surface of the magnetized specimen. These particles are attracted by the magnetic field gradients in the vicinity of flaws and tend to adhere to the surface in such regions, thus giving visible indications of the presence of flaws. The powder of iron particles can be applied in a dry form or suspended in a liquid which is poured over the specimen and allowed to dry. Dry powders are more effective for subsurface flaws and are more convenient for inspection under field conditions. The wet method is usually superior for detecting fine and shallow flaws. Often the particles are colored to give good color contrast with the surface being inspected. Disadvantages of the magnetic particle method are the requirement for visual inspection of surfaces that are not easily accessible and the absence of a permanent, quantitative record of the inspection.

In addition to the magnetic powder, there are two other methods called magnetographic and magnetometric. The magnetographic method is an indirect approach which is especially applicable to irregular geometries. This approach utilizes magnetic tape which is pressed to the specimen, thereby picking up a magnetic "imprint" of any leakage fields present. The tape is later scanned with a magnetometer. The magnetometric detection methods are generally used to directly scan a specimen, thereby providing a map of the leakage field produced by a defect.

The Barkhausen effect, another NDE technique, depends on Barkhausen noise from various material properties including applied and residual stress, grain size, carbon content, phase morphology, and precipitate size and distribution. (Ref. 7). In a ferromagnetic material, the interaction of an applied magnetic field occurs at the atomic level according to the experimentally verified magnetic domain theory. The interaction of magnetic domain walls with dislocations, grain boundaries, precipitate particles, etc., under the application of an externally applied magnetic field of slowly varying intensity, may be sensed by appropriate detection means (inductive, optical, or acoustic sensors). Most of the effort to date has been directed toward applications involving residual stress measurement, however, research in recent years has also demonstrated the applicability of the method for the NDE of a variety of material properties, such as grain size and orientation, defect structure, and metallurgical composition.

Barkhausen noise measurement for NDE has the following advantages: (1) the measurement is fast - a single measurement taking only a few seconds; (2) usually no preparation of the specimen, such as surface cleaning, is required; (3) the result is objective; (4) a quick survey of large objects is possible; (5) fast feedback to process control is possible in many cases; and (6) the method is entirely nondestructive.

Barkhausen noise method has the following limitations: (1) with the inductive method, only a thin surface layer (0.5 mm) is measured; (2) the thickness and geometry of the sample may affect the results; (3) calibration may be required to compare results from samples of different thicknesses and geometrics; (4) the result is dependent on several microstructural parameters, and changes in one factor may completely overshadow changes in others.

The fact that the Barkhausen signal is affected by a number of material properties complicates reliable interpretation of experimental results. Lacking is a fundamental understanding of the influence that various microstructural properties and defect structures have on the details of the dynamical domain processes. While the Barkhausen Effect has been used successfully in a number of situations, development is needed in order to easily apply this technique. For that reason, this NDE technique will not be choosen for detail application to the tank car damage assessment problem.

Radiography, using x-rays or gamma rays, is the most popular NDE technique (Ref. 8) In this procedure, the radiation source directs radiation through the object and onto photographic film. The level of radiation is attenuated according to the type and mass of the object's material content. If a flaw is present, the radiation path length is changed and an image of the flaw is formed on the film. This use of radiography has advantages in terms of sensitivity, resolution, and the creation of a permanent record. The most recent development in radiography includes some forms of automation where the image is translated to a television monitor and there is evidence that for some applications the use of photographic film can be eliminated all together.

Unfortunately, the use of x-rays or gamma

[6] *Beissner, R.E., en tal, "NDE Applications of Magnetic Leakage Field Methods, A State-Of-The-Art Survey", NTIAC-80-1, January 1980, Southwest Research Institute, San Antonio, Texas 78284*

[7] *Matzkanin, G.A., en tal, "The Barkhausen Effect and Its Applications to Nondestructive Evaluations", NTIAC-79-2, October 1979, Southwest Research Institute, San Antonio, Texas 78284*

[8] *Gardner, G. C., "Automated Radiography - A State-Of-The-Art Survey", NTIAC-78-1, June 1978, Southwest Research Institute, San Antonio, Texas 78284*

rays requires that the photographic film or some other image receptor be on the opposite side of the item to be evaluated from the radiation source. In the case of the damaged tank car, the interior of the car will not be assessable, thus, radiography cannot be used. However, this NDE technique will be useful for verifying other NDE techniques being studied and may be a recommended procedure for application in manufacturing processes or the shop repair of damaged tank cars.

Another type of NDE technique concerns the effect on materials placed on the surface of the specimen to be tested. One of these materials is composed of liquid crystals (Ref. 9). The most useful characteristic of liquid crystals is their change in color as a function of temperature. The heat which causes the change is due to the existence of a flaw in the specimen, therefore, the existence and location of such flaws can be detected. Another procedure is the use of a dye penetrant which can be used to locate small surface cracks in the specimen which are normally not visible. The dye is painted onto the specimen and the dye penetrates any cracks present. The dye is then wiped off and a different material is brushed on. The dye from the cracks interacts with the second material and a visible portrayal of the existing cracks is generated. These types of NDE techniques have a limited application in the tank car evaluation problem in that both require a visible technique for studying the result and are not amendable to automation. However, both will be used under certain circumstances in this study as a means of verifying other techniques and used in the analysis of intermediate type tests on certain specimens.

Other NDE techniques depend on electromagnetic radiation emitted by the object in question or reflected from the object. The latter of course includes the visible inspection of the object where a properly trained person can conclude a great deal about the condition of the tank car by simply observing the damage and comparing with knowledge gained from past experience. This type of evaluation can be enhanced by the use of appropriate tools such as telescopes, lighting, and comparison standards for determining alignment and the level of deformation. This concept can be improved by determining in detail the level of deformation (dent radius mapping) through the use of Moire patterns projected optically on a surface. In addition, laser surveying instruments can be used to measure relative deformations precisely. The former concept of radiation emission includes the emission of electromagnetic radiation due to the object's temperature. The amplitude and frequency spectra depend on the temperature level and on the object's surface emissivity. At temperatures below incandescence, the emitted radiation is in the infrared and longer wavelength regions of the spectrum. A device which can detect infrared emission can indicate relative hot and cold spots which in turn can be interpreted in terms of size and location of a leak. Therefore, infrared techniques will be studied closely for the purpose of detecting leaks prior to the removal of the damaged tank car and the formation of leaks during the removal operation.

[9] *Ash, J. Ivan, "Liquid Crystals For Nondestructive Evaluation", NTIAC-78-2, September 1978, Southwest Research Institute, San Antonio, Texas, 78284*

## IMPACT DATA ON FLAT PLATES

The solution to the damaged tank car assessment problem requires knowledge in at least two specific areas. One is the development of a data base which can serve as basic information as to how tank car materials respond to dynamic impacts. That is, once the damage has been sustained, what are the characteristics of the types of damage which can be used to predict potential rupture of the tank car? The other is to apply NDE techniques on sample-damaged materials in order to determine their effectiveness in locating and identifying specific types of flaws. As an initial phase in the program, flat plates made of steel with properties exceeding the American Society for Testing and Materials (ASTM) Standards for tank car steel were impacted using the FRA/BRL Drop Hammer Facility. These impacts produced various degrees of damage in the form of dents and fractures.

Figure 1 presents a view of the FRA/BRL Drop Hammer Facility. The hammer is a massive weight

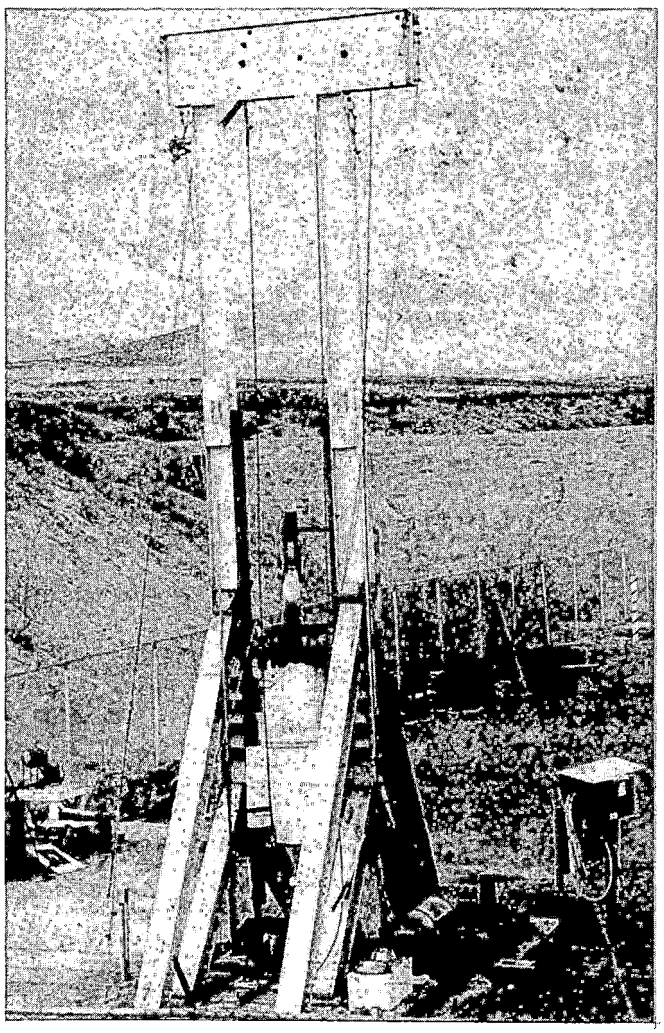

Figure 1: The FRA/BRL Drop Hammer Facility

of 4,574 kgm (10,084 lbs) which is raised vertically to some predetermined height depending on the amount of kinetic energy desired on impact. The hammer is raised by a cable attached to its top end with a special hook which allows the hammer to drop with a minimum of delay once the procedure is initiated. This mechanism is referred to as the quick release. To trigger the quick release, a pin is pulled from its initial position by a device called an actuator. The actuator pulls on the pin gradually due to a hydraulic pump hand worked by a technician. A device which records the velocity of the hammer is called the comb. The data generated by the comb and associated accelerometers are fed directly into a computer and serve as basic data from which calculations are performed. The calculational results consist of acceleration of the hammer as a function of time and residual hammer energy following a punch through of the test specimen.

A diagram of the interacting parts which creates the damage is presented in Figure 2. The hammer does not impact the material, but has an object called a tup attached to the striking end. The tup is threaded to the hammer and can be of arbitrary shape and size. In the figure, the striking surface of the tup is shown to be flat with the tip consisting of a layer of hardened steel. Below the flat surface of the tup in the diagram is the die which is also composed of hardened steel. The die is held in place by a die holder which lies in a recess carved in the heavy steel base on which the entire structure is attached. If the tup perforates a plate, it can pass through the opening in the die. The cutting edge of the die was rounded off to yield more realistic results.

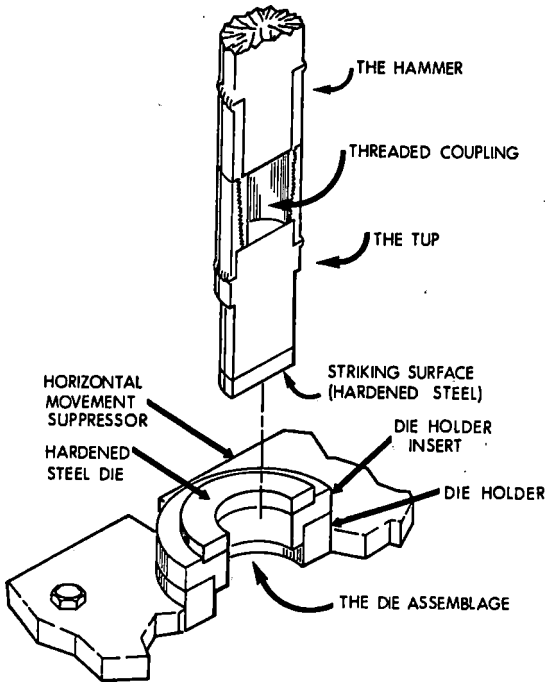


Figure 2: The Tup and Die Assemblage of the FRA/BRL Drop Hammer Facility

Since the purpose of these tests was to obtain a variety of types and levels of damage, both the tup and the die sizes were varied. The three tup sizes used were 5.08 cm (2 inch), 9.525 cm (3.75 inch), and 13.97 cm (5.5 inch). Some of the tests were conducted with a flat tup, but most tests were performed using a hemispherical tup. The four die sizes used were 14.24 cm (6.0 inch), 20.96 cm (8.25 inch), 27.94 cm (11.0 inch, and 34.93 cm (13.75 inch).

The plates were made of steel with the following characteristics: ASTM A515, Grade 70, Minimum tensile strength of $4.9217 \times 10^7$ Kgs/m$^2$, Minimum elongation in 5.08 cm (2 inches) of 20%. Their thicknesses were 1.5875 cm (5/8 inches) with a surface size of 60.96 cm (24 inches) square. The Brinell Hardness (BH) of each of the plates was measured and is included as the last three digits in a Identification Number (ID) associated with each plate.

For those plates where the tup did not punch through or cause a massive tear, the depth of the dent was measured using a dial micrometer (DM). A typical sample of a DM measurement of a plate is presented in Figure 3. The abscissa in the figure represents positions along a diagonal of the square plate with one corner being zero and the maximum value of 86.36 cm (34 inches) being the opposite plate corner. The die diameter and therefore the position of the die relative to the plate was determined by assuming that the die was centered in the same position as the deepest point in the dent. The tup was located in the same manner.

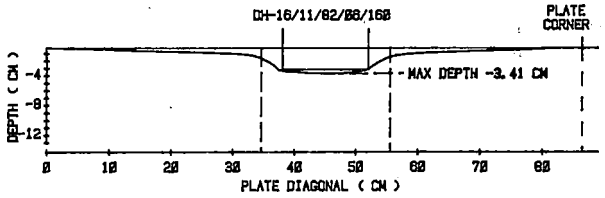


Figure 3: Sample Plot of DM Measurements

Nine tests were conducted using the flat tup with a diameter of 13.97 cm (5.5 inches). The symbol designation for this tup is $T_{LF}$. A summary of the die diameters and hammer heights for these tests is presented in Table 1. The three die diameters used were 15.24 cm (6.0 inches), 20.96 cm (8.25 inches), and 27.94 cm (11.0 inches). For this tup and the 15.24-cm die, the primary failure mechanism is shear with the tup penetrating the plate in a punching type action. Figure 4 presents a view of the plate following Test Number 2 (DH-16-11-82-03-136) where there was a complete punch through. The hammer height (HH) was 82.55 cm (32.5 inches. By reducing the HH by 1.27 cm (0.5 inches), the tup failed to punch through as shown in Figure 5

and Figure 6 for Test Number 1 (DH-16-11-82-02-145). Figure 5 presents the flat impression corresponding to the flat tup on the impact side of the plate. The flat bulge on the bottom side is shown in Figure 6. Even though this test was nearly a punch through, there were no visible cracks or tears.

TABLE 1: $T_{LF}$ IMPACT TESTS SUMMARY

| Test No. | Identification Number | Die Diameter (cm) | Hammer Height (cm) |
|---|---|---|---|
| 1 | DH-16-11-82-02-145 | 15.24 | 81.28 |
| 2 | DH-16-11-82-03-136 | 15.24 | 82.55 |
| 3 | DH-16-11-82-01-153 | 15.24 | 83.82 |
| 4 | DH-16-11-82-04-153 | 20.96 | 86.36 |
| 5 | DH-16-11-82-05-134 | 20.96 | 91.44 |
| 6 | DH-16-11-82-06-160 | 20.96 | 96.52 |
| 7 | DH-16-11-82-07-167 | 20.96 | 101.60 |
| 8 | DH-16-11-82-08-175 | 27.94 | 106.68 |
| 9 | DH-17-11-82-01-198 | 27.94 | 111.76 |

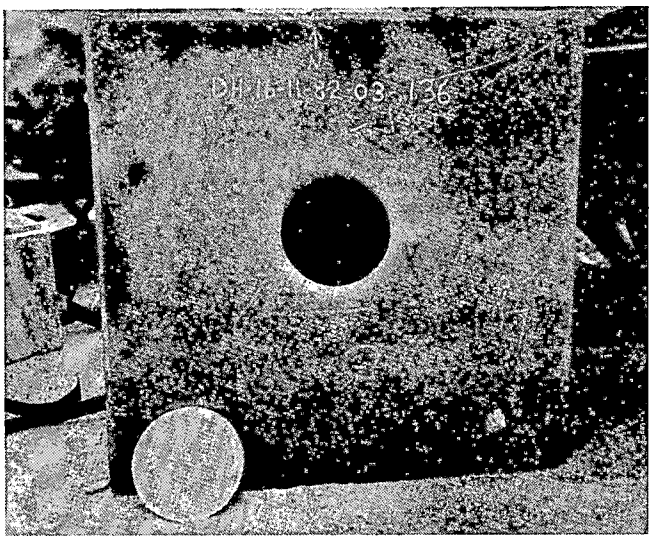

Figure 4: $T_{LF}$ Impact Test Plate From Test No. 2

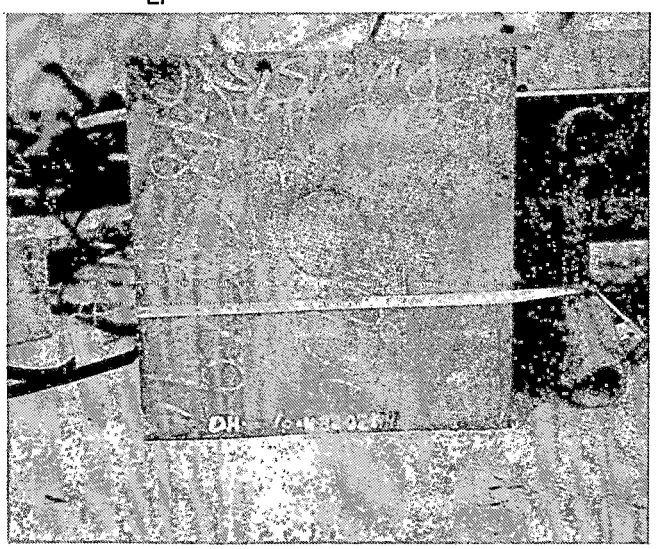

Figure 5: Impact Side of Plate From Test No. 1

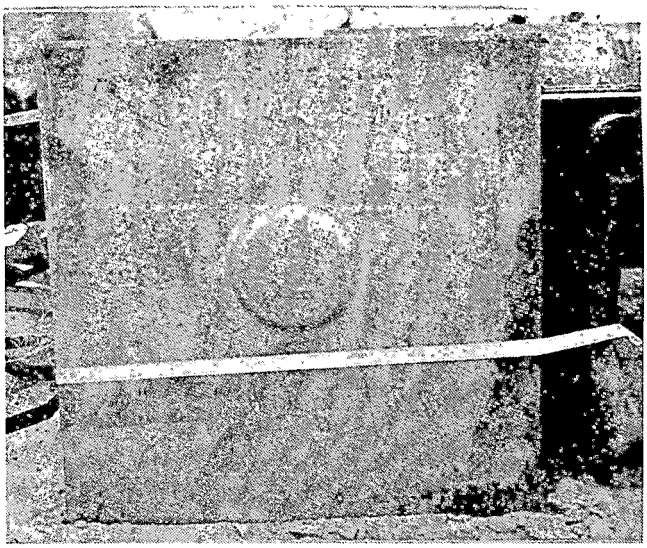

Figure 6: Bottom Side of Plate From Test No. 1

The DM measurements for Test Number 1 are presented in Figure 7. The diameter of the bottom of the dent, measured from the plot, is less than the diameter of the tup, an apparent contradiction. However, when the tup fails to perforate the plate, the hammer rebounds and at the same time the plate contracts due to elasticity.

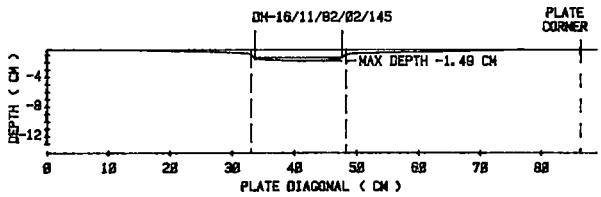


Figure 7: DM Measurements for Test Number 1

A plot of the maximum dent depth as a function of potential energy (hammer height)-presented area of the die ratio is presented in Figure 8. The rate of dent depth increase is greater for the larger die diameters. This is attributed to a tendency toward the bending mode response as the distance between the tup edge and the die edge increases.

The hemispherical shape was considered more representative for general purposes than the flat shape, thus the remaining impacts were performed using hemispherical tups. The three hemispherical tup sizes used were 13.97 cm (5.5 inches) ($T_{LH}$), 9.525 cm (3.75 inches) ($T_{MH}$), 5.08 cm (2 inches) ($T_{SH}$). It was anticipated that the data would show that the dent producing capability of these tups would exceed flat tups of the same diameters dropped at the same HH values. The reason is that the initial area of contact

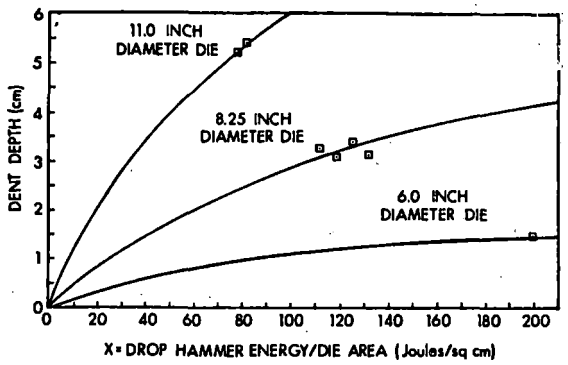


Figure 8: Dent Depth Versus Potential Energy-Die Area Ratio for $T_{LF}$ Test Data

between the tup and the plate constitutes a point, thus, the force per unit area is far greater during the early portion of the tup-plate interaction. Also the distance between the tup and the edge of the die is greater, thus, the plate response tends away from the shear mode and toward the bending mode.

The $T_{LH}$ tup was used in 24 tests which are listed in Table 2. The four die diameters used were 15.24 cm (6.0 inches), 20.96 cm (8.25 inches), 27.94 cm (11.0 inches), and 34.92 cm (13.75 inches). For each of the die diameters, the hammer was raised to a height of 25.4 cm (10 inches) on the first drop and progressively raised in following tests until the tup perforated the plate (caused a large crack or tear). The hammer facility failed on Test Number 21, thus, no data was obtained in that test. The tup perforated the plates on Test Numbers 15, 25, 32, and 33.

TABLE 2: $T_{LH}$ IMPACT TESTS SUMMARY

| Test No. | Identification Number | Die Diameter (cm) | Hammer Height (cm) |
|---|---|---|---|
| 10 | DH-26-04-83-03-160 | 15.24 | 25.40 |
| 11 | DH-26-04-83-04-160 | 15.24 | 50.80 |
| 12 | DH-17-11-82-02-131 | 15.24 | 96.52 |
| 13 | DH-17-11-82-03-126 | 15.24 | 106.68 |
| 14 | DH-26-04-83-05-160 | 15.24 | 127.00 |
| 15 | DH-26-04-83-06-160 | 15.24 | 127.80 |
| 16 | DH-26-04-83-01-160 | 20.96 | 25.40 |
| 17 | DH-26-04-83-02-160 | 20.96 | 76.20 |
| 18 | DH-18-11-82-09-149 | 20.96 | 127.00 |
| 19 | DH-18-11-82-10-126 | 20.96 | 152.40 |
| 20 | DH-18-11-82-11-149 | 20.96 | 177.80 |
| 21 | DH-18-11-82-12-140 | 20.96 | 228.60 |
| 22 | DH-25-04-83-20-160 | 27.94 | 25.40 |
| 23 | DH-25-04-83-21-160 | 27.94 | 76.20 |
| 24 | DH-25-04-83-22-160 | 27.94 | 127.00 |
| 25 | DH-25-04-83-23-160 | 27.94 | 177.80 |
| 26 | DH-25-04-83-16-160 | 34.92 | 25.40 |
| 27 | DH-25-04-83-17-160 | 34.92 | 76.20 |
| 28 | DH-25-04-83-18-160 | 34.92 | 127.00 |
| 29 | DH-25-04-83-19-160 | 34.92 | 177.80 |
| 30 | DH-26-04-83-15-160 | 34.92 | 203.20 |
| 31 | DH-26-04-83-16-160 | 34.92 | 203.20 |
| 32 | DH-27-04-83-01-160 | 34.92 | 203.20 |
| 33 | DH-27-04-83-02-160 | 34.92 | 203.20 |

Even though the tup had a hemispherical shape, a shear plug was formed in Test Number 15. Photographs of the result are presented in Figures 9 and 10. In that test, the die diameter was 15.24 cm (6.0 inches) and the HH value was 178 cm (70 inches). The perforation was not a clean punch through so the plug and tup jammed in the die.

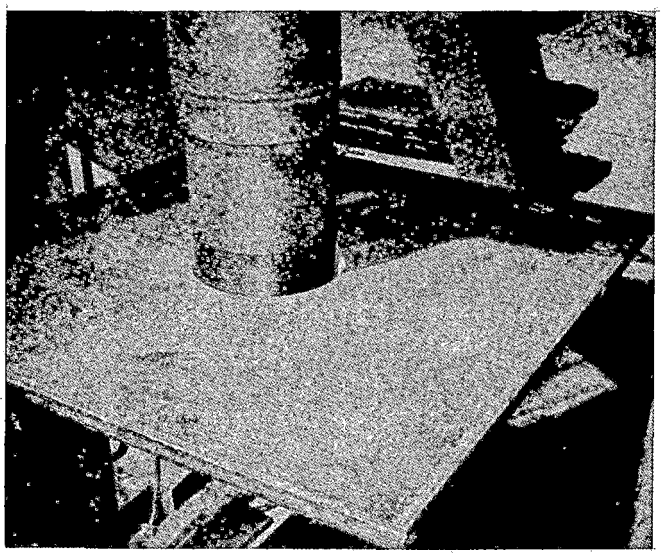

Figure 9: Impact Side of Plate From Test No. 15

Figure 10: Bottom Side of Plate From Test No. 15

A representative sample of a perforation is presented in Figures 11 and 12. The test in question is Test Number 25 where the die diameter was 27.94 cm (11.0 inches) and the HH was 178 cm (70 inches). The large crack appeared to have started on one side of the bulge and then propagated circumferencially. The damage mechanism appears to have been a severe thinning of the steel around the sides of the bulge with the thinned metal eventually separating by ductile fracture.

Figure 13 is a sample plot of the DM measurements of those plates which were not perforated in this group of tests.

Figure 11: Impact Side of Plate From Test No. 25

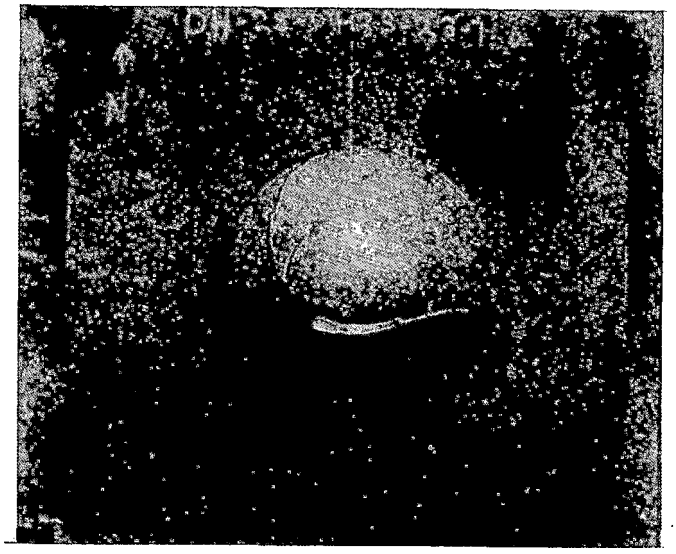

Figure 12: Bottom Side of Plate From Test No. 25

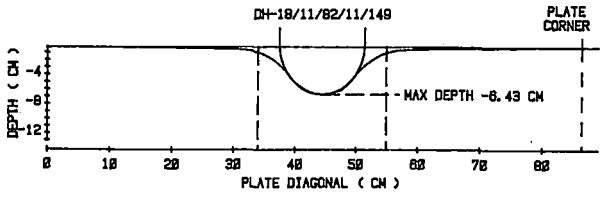


Figure 13: DM Measurements For Test Number 20

The dent depth as functions of drop hammer energy-die area ratio for those tests without perforations are presented in Figure 14. While the trends are similar to the flat tup data (Figure 8), the dent depths are greater as a function of the potential energy-die ratio. Again, the rate of dent depth increase is greater as the larger dies were used.

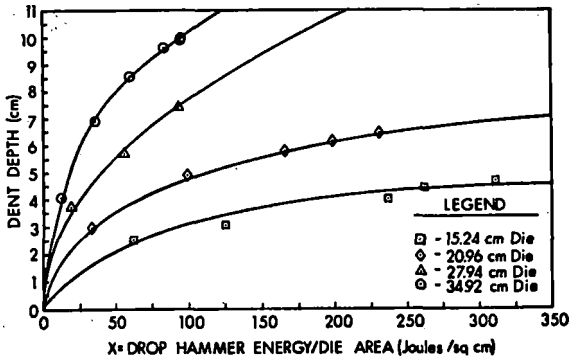


Figure 14: Dent Depth Versus Potential Energy-Die Area Ratio for $T_{LH}$ Test Data

The next group of tests were done using the $T_{MH}$ tup. In general it was expected that the response by the plates would be similar to the previously discussed group, but that the dent depths would be greater for equal values of hammer heights. A summary of these tests are listed in Table 3.

TABLE 3: $T_{MH}$ IMPACT TESTS SUMMARY

| Test No. | Identification Number | Die Diameter (cm) | Hammer Height (cm) |
|---|---|---|---|
| 34 | DH-25-04-83-01-160 | 15.24 | 25.40 |
| 35 | DH-25-04-83-02-160 | 15.24 | 50.80 |
| 36 | DH-25-04-83-03-160 | 15.24 | 76.20 |
| 37 | DH-25-04-83-04-160 | 15.24 | 101.60 |
| 38 | DH-25-04-83-05-160 | 20.96 | 25.40 |
| 39 | DH-25-04-83-06-160 | 20.96 | 50.80 |
| 40 | DH-25-04-83-07-160 | 20.96 | 76.20 |
| 41 | DH-25-04-83-09-160 | 27.94 | 25.40 |
| 42 | DH-25-04-83-10-160 | 27.94 | 50.80 |
| 43 | DH-25-04-83-12-160 | 34.92 | 25.40 |
| 44 | DH-25-04-83-13-160 | 34.92 | 50.80 |
| 45 | DH-25-04-83-14-160 | 34.92 | 76.20 |

Figures 15 and 16 presents photographs of the impact side and the bottom side of a sample plate where the $T_{MH}$ tup was used. The response of the plate was similar to that obtained for the larger hemispherical tup. Figure 17 presents a sample of the DM measurements for this group of tests, which is also similar to the previously discussed group. The dent depth as functions of drop hammer energy/die area ratio are presented in Figure 18. The trends are similar to the those of the previous group of tests, but the dent depths are greater.

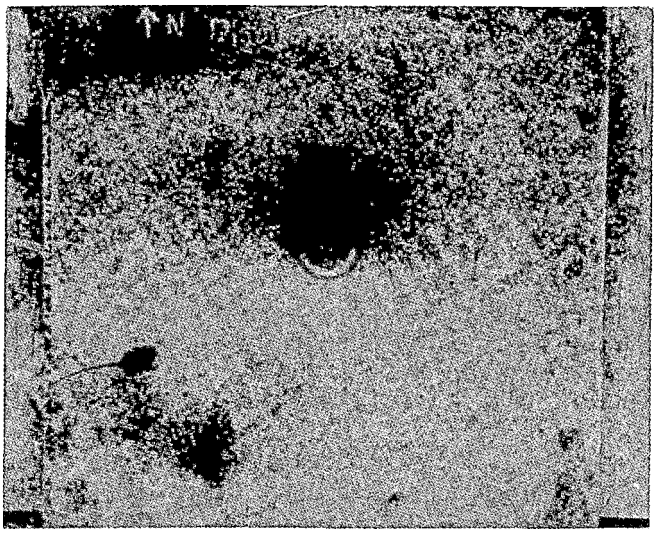

Figure 15: Impact Side of Plate From Test No. 40

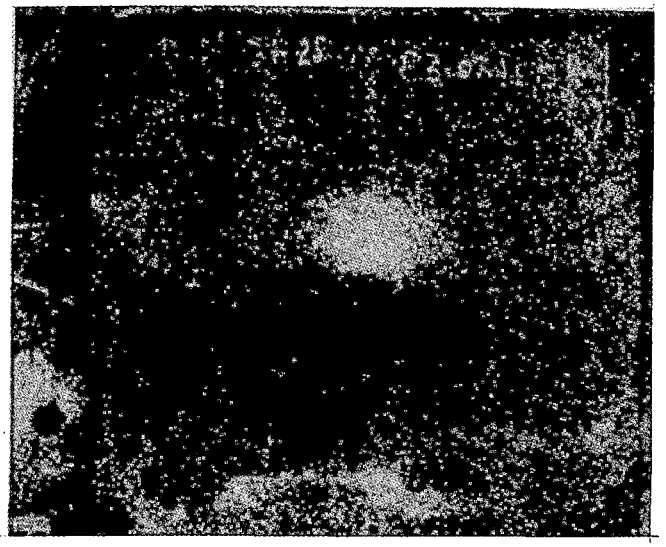

Figure 16: Bottom Side of Plate From Test No. 40

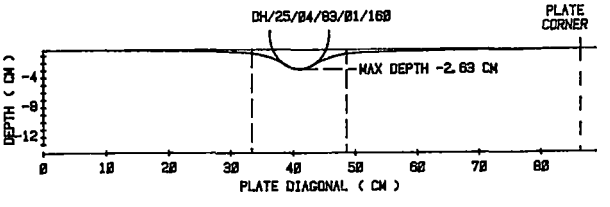


Figure 17: DM Measurements For Test Number 34

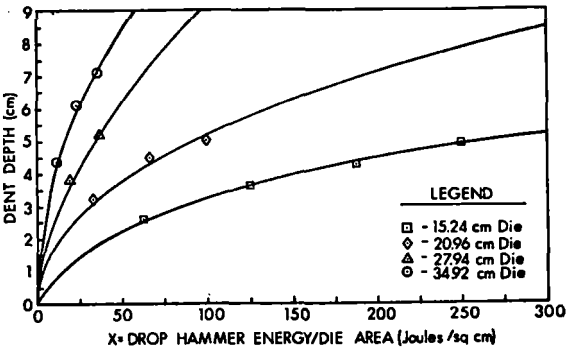


Figure 18: Dent Depth Versus Potential Energy-Die Area Ratio for $T_{MH}$ Test Data

The remaining tests were performed using the $T_{SH}$ tup. Table 4 presents a summary of the tests conducted. Photographs of the impact side and the bottom side of a plate from a sample test are presented in Figures 19 and 20 respectively. Figure 21 presents a sample of the DM measurements which shows that the plates experienced a great deal of bending due to the relatively large amount of material between the edge of the die and the tup.

TABLE 4: $T_{SH}$ IMPACT TESTS SUMMARY

| Test No. | Identification Number | Die Diameter (cm) | Hammer Height (cm) |
|---|---|---|---|
| 46 | DH-26-04-83-07-160 | 15.24 | 10.16 |
| 47 | DH-26-04-83-08-160 | 15.24 | 20.32 |
| 48 | DH-17-11-82-04-140 | 15.24 | 30.48 |
| 49 | DH-17-11-82-05-167 | 15.24 | 33.02 |
| 50 | DH-17-11-82-06-167 | 15.24 | 35.56 |
| 51 | DH-17-11-82-09-147 | 15.24 | 38.10 |
| 52 | DH-17-11-82-07-167 | 15.24 | 40.64 |
| 53 | DH-17-11-82-08-136 | 15.24 | 43.18 |
| 54 | DH-26-04-83-09-160 | 20.96 | 10.16 |
| 55 | DH-26-04-83-10-160 | 20.96 | 20.32 |
| 56 | DH-18-11-82-01-179 | 20.96 | 30.48 |
| 57 | DH-17-11-82-12-171 | 20.96 | 33.02 |
| 58 | DH-17-11-82-11-157 | 20.96 | 40.64 |
| 59 | DH-17-11-82-10-167 | 20.96 | 45.72 |
| 60 | DH-26-04-83-11-160 | 27.94 | 10.16 |
| 61 | DH-26-04-83-12-160 | 27.94 | 20.32 |
| 62 | DH-18-11-82-04-160 | 27.94 | 30.48 |
| 63 | DH-18-11-82-03-179 | 27.94 | 33.02 |
| 64 | DH-18-11-82-02-171 | 27.94 | 35.56 |
| 65 | DH-26-04-83-13-160 | 34.92 | 10.16 |
| 66 | DH-26-04-83-14-160 | 34.92 | 20.32 |
| 67 | DH-18-11-82-08-167 | 34.92 | 33.02 |
| 68 | DH-18-11-82-05-171 | 34.92 | 35.56 |
| 69 | DH-18-11-82-07-163 | 34.92 | 35.56 |
| 70 | DH-18-11-82-06-160 | 34.92 | 38.10 |

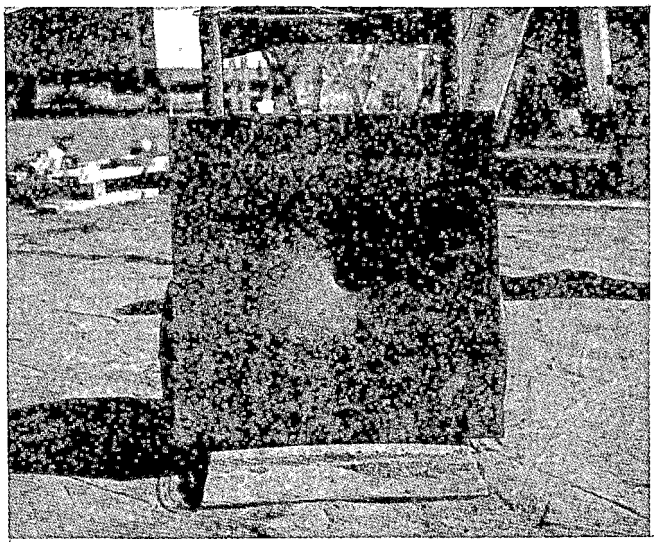

Figure 19: Impact Side of Plate From Test No. 69

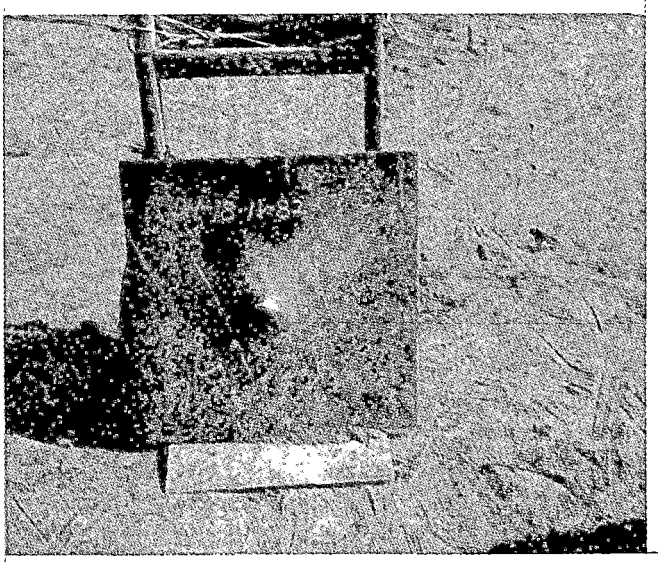

Figure 20: Bottom Side of Plate From Test No. 69

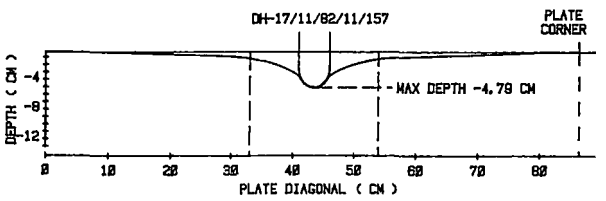


Figure 21: DM Measurements For Test Number 58

In practically all of the $T_{SH}$ tup tests visible cracks were observed on the bottom side of the plates on or near the apex of the bulges. The seriousness of these types of cracks with respect to a tank car rupture cannot be estimated with current knowledge. However, this data indicates that for a bend of radius 2.54 cm (1.0 inch) and a dent depth of 3.81 cm (1.5 inches) to 6.35 cm (2.5 inches), there will probably be surface cracking of the steel on the inside of the tank car. By continuing this process of relating steel damage to the characteristics of dents, a means of assessing the damage may be developed. In all of this test data, the additional complication of having a weld in the dent has not been addressed. Welds will have to be included in the final procedures for the assessment of damaged tank cars.

Figure 22 presents the plot of the dent depth as functions of drop hammer/die area ratio for the test results where the $T_{SH}$ tup was used. The trends are similar to those where the data was generated with the larger hemispherical tups.

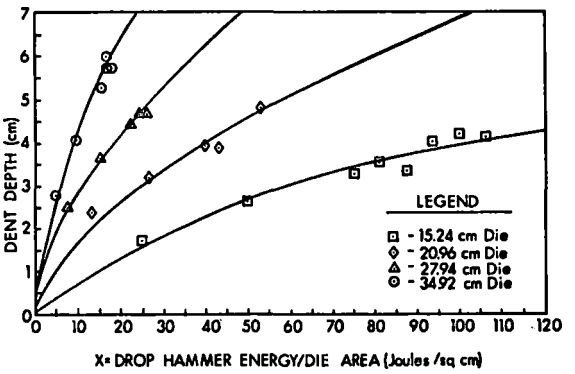


Figure 22: Dent Depth Versus Potential Energy-Die Area Ratio for $T_{SH}$ Test Data

As with any test program, in the event the data scales a great deal of future test reduction may be realized. Consequently an attempt to scale the dent depth as a function of drop hammer energy-die area ratio was pursued. The results of this effort are presented in Figure 23. As Figure 23 shows, the scaling was done by nondimensionalizing the parameters. The X and Y parameters are defined as follows:

$$X = \{\{E/S\} * \{D_T/D_D\}\}^{1/2}$$

and

$$Y = \{DD/d\} * \{D_T / D_D\}^{1/4}$$

where: $D_T$ is tup diameter,
DD is depth of dent (cm),
d is plate thickness (1.5875 cm = 5/8 in.),
$D_D$ is die diameter (cm),
E is plate density times tup velocity squared (kg/m-sec squared),
S is ultimate strength of plate material ($4.48 \times 10^8$ kg/m-sec squared= 65,000 psi), and
the density of the steel was assumed to be equal to 7.78 gm/cc.

This model can be used to interpolate, but to extrapolate involves unknown risks. In the event the model is used to extrapolate to other conditions, tests at those conditions will be required for verification.

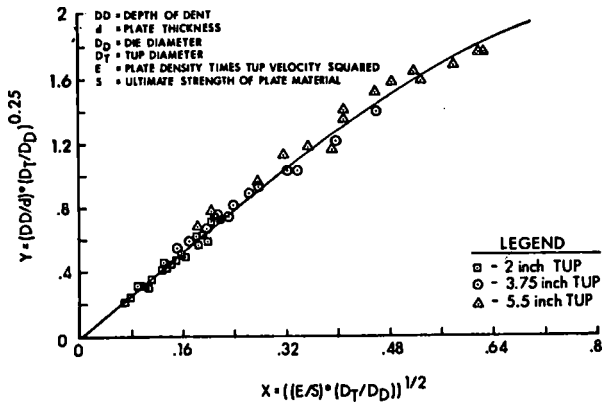


Figure 23: Nondimensional Presentation of the Dent Depth Versus Energy for the Hemispherical Tup Impacts

NDE OF 1/5 SCALE RAILROAD TANK CAR

NDE techniques were applied to tank car type steel for the purpose of evaluating available NDE procedures by the Nondestructive Test Group of the Materiel Testing Directorate (MTD), Aberdeen Proving Ground, Maryland. (Ref. 10). The MTD agreed to evaluate a 1/5 scaled tank car model which had been impacted and three of the damaged plates discussed in the last section. The two NDE techniques used were ultrasonics and a form of the Magnetic Leakage Field Method. The objective was to locate existing discontinuities indicative of cracks in the 1/5 scale tank car model and the three plates. These data were then to be used to determine the ability of the NDE techniques used to evaluate the inward and outward sides of a damaged tank car from the outside.

The inspection was done with the Fluorescent Magnetic Particle Wet Continous Method and the Ultrasonic Pulse Echo Contact Method (Shear Wave Model). In the former, the items were magnetized using direct current, sprayed with a bath consisting of size 14A fluorescent magnetic particles (Magnaflux Corp.) suspended in a petroleum distillate liquid vehicle (light oil petroleum distillate), and inspected under blacklight for patterns indicative of cracks or other defects. In the latter, a Krautkramer Model USIP-11 flaw detector unit was used with ceramic, 1/4 inch square, 45 degrees angle beam, 2.25 MHz and 10 MHz transducers calibrated to the sound path in an IIW reference test block. Ninety-weight gear oil and artillery grease were used for the transducer couplant. The unit sensitivity level was adjusted to produce a 100% full screen height echo from the IIW test block with a 10.2 cm (4 inch) referenced distance.

A side view of the 1/5 scale model tank car and an end view are presented in Figures 24 and 25, respectively. The latter view shows the dent in the end which was photographed. The dented ends of the model and the bulged section of the three plates were inspected by the magnetic particle (direct contact, coil, and electric magnet contour probe) and ultrasonic methods. The 10 MHz transducer was used to inspect the thin 1/5 scale tank (approximately 3 mm thick) and the 2.25 MHz transducer for the thicker sample plates (approximately 15 mm thick) for better resolution.

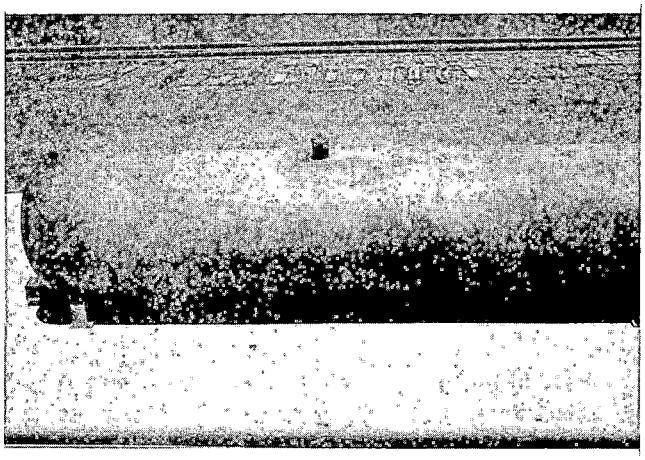

Figure 24: The 1/5 Scale Tank Car Model

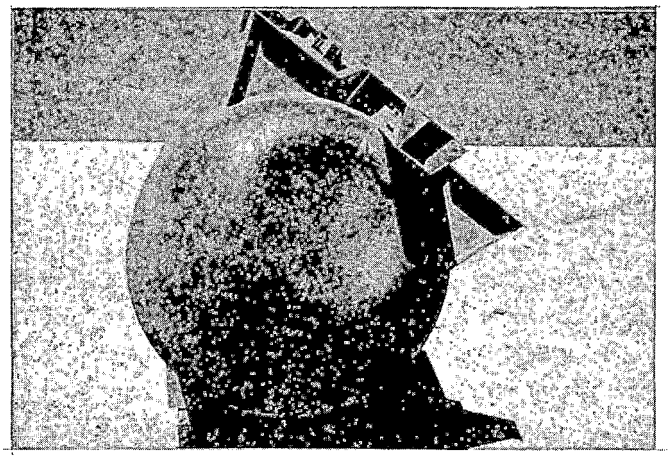

Figure 25: A Damaged End of the 1/5 Scale Tank Car Model

No discontinuities indicative of cracks were evident in two sample plates (Numbers DH-18-11-82-04-160 and DH-18-11-82-01-179) and the 1/5 scale model. The sample plate Number DH-18-11-82-06-160 contained 4 cm and 1.1 cm length magnetic particle crack patterns on the back side. The patterns were nearly identical using contacts, coil, or electric magnet. The patterns using the contact method are shown in Figure 26. Both crack indications can be detected from either side of the plate with ultrasonics. The ultrasonic inspection from the front side of the plate produced a 100 % full scale height back echo from the larger crack and a 55 % full scale height echo from the smaller cracks (see Figures 27 and 28)

[10] *Yocum, Russell, "NDT of Damaged 1/5 Scale Railroad Tank Car", Report No. 83-N-4, June 29, 1983, Materiel Testing Directorate, Aberdeen Proving Ground, Maryland 21005*

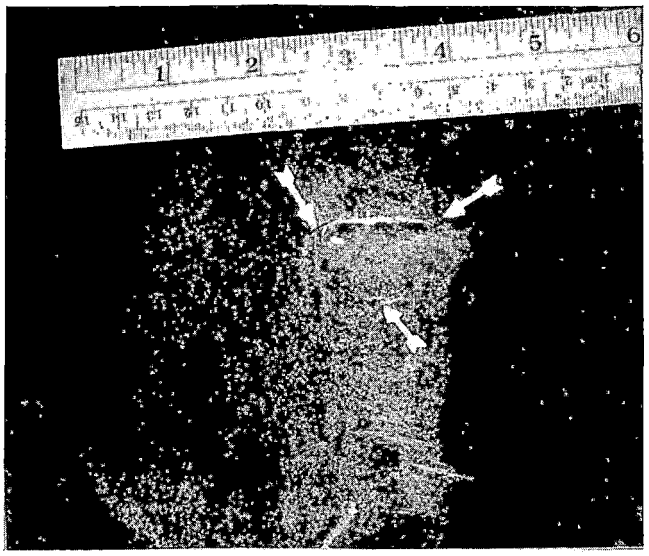

Figure 26: Magnetic Particle Crack Patterns on Plate Number DH-18-11-82-06-160

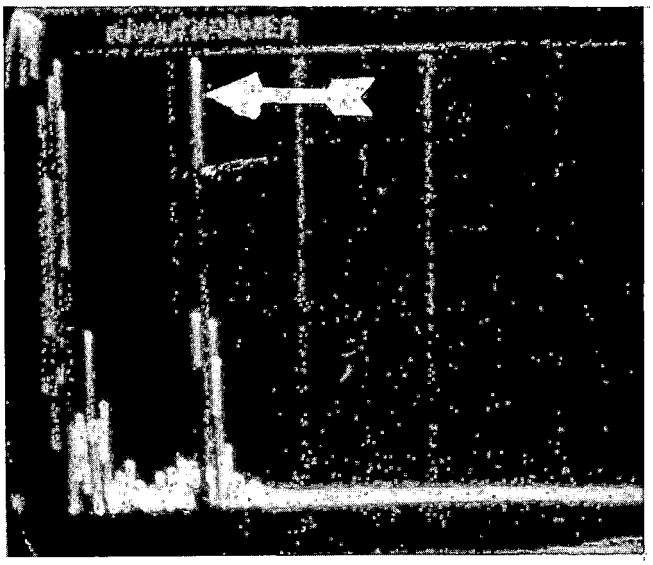

Figure 27: Ultrasonic Inspection Indication of 4 cm Crack Pattern

Several irrelevant ultrasonic multiple echoes were produced at the same height and approximate location as the smaller crack, therefore, this is the smallest detectable size for the ultrasonic instrumentation. The 2.25 MHz transducer produced a better presentation than the 10 MHz transducer in the actual thickness sample.

The study produced two conclusions as follows: (1) The Fluorescent Magnetic Particle Wet Continuous Method could only detect discontinuities on the exposed exterior surface and would be of no use in locating discontinuties indicative of cracks or other defects on the inward surface. (2) The Ultransonic Pulse Echo Contact Method (Shear Wave Mode) could locate discontinuities throughout the thickness of the tank wall (inside and outside).

Ultrasonics was recommended for use as the main inspection method and those areas which can-

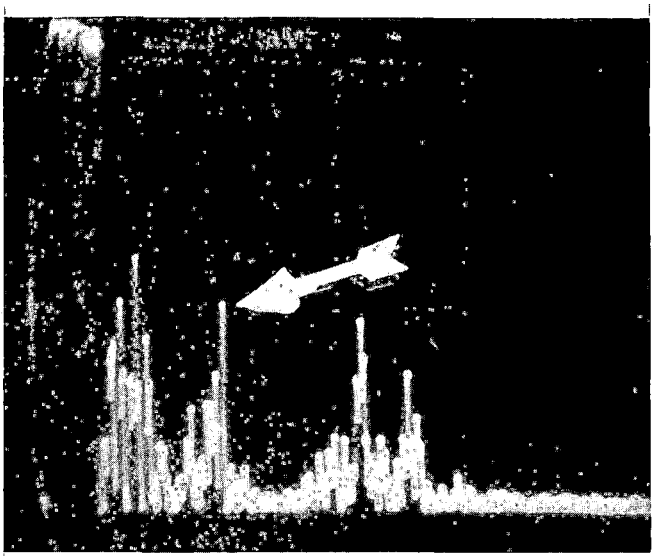

Figure 28: Ultrasonic Inspection Indication of 1.1 cm Crack Pattern

not be ultrasonically inspected (due to the shape of the area), that magnetic particle inspection technique be used (with a permanent magnetic or electric contour probe). The 10 MHz transducer is not needed to inspect a full scale tankcar, thus, a 2.25 MHz transducer was recommended.

## PARALLEL NDE STUDIES

The Idaho National Engineering Laboratory (INEL) assisted in the program and the material in this section constitutes the major points of that participation. (Ref. 11)

Three general characteristics of NDE techniques which are needed for application to the tank car damage assessment problem were identified. These are: (1) Remoteness and Quickness- "Remote sensing should be used to the maximum extent possible for the safety of personnel. Due to the fact that the situation may be developing rapidly, there should be an emphasis on speed, immediacy, and timeliness of the information to be gathered." (2) Accurate Determinations - "Due to the high potential for loss of lives and property, an accurate determination of the condition of the tank car is required. A significant body of basic metallurgical, stress, structural, and historical data need to be developed and made available for correlation in the field with NDE findings." (3) Portability - "Techniques employing equipment or information which cannot be assembled on the accident site immediately will contribute little to the required assessment. The need for portability places a constraint on the various techniques which can be employed, and requires development of an overall systematic approach." The investigation and development of NDE techniques and procedures for evaluating damaged tank cars will be guided by

[11] *Beller, L.S., en tal, "Survey of Nondestructive Methods for Evaluating Derailed Tank Cars," BRL Contract Report to be published, Ballistic Research Laboratory, Aberdeen Proving Ground, Maryland 21005-5066*

these basic and fundamental guidelines.

INEL made an independent survey of the various NDE techniques available which culminated in a tenative list of NDE techniques which it is anticipated can be the most useful. This tenative list consist of the following:

(1) "The NDE techniques suitable for the initial remote assessment and for determining the safety of approaching the tank car are: (a) Supported visual observation and inspection, as defined. These are to determine gross conditions of damage, to determine and measure larger deformations, and assess general condition and safety. (b) Infrared imaging - to determine existence, location, and relative sizes of significant leaks.

(2) The NDE techniques for detailed assessments at close range or in contact with the damaged tank car are: (a) Supported visual examination. to find finer details and general observations not possible from remote locations. (b) Ultrasonics to make thickness measurements as an index to local deformation, detect cracks, and related defects in critical and/or deformed areas, and (potentially) parameters related to metallurgical variables of concern to safety of continuing further operations. (c) Acoustic Emission devices to be installed immediately on close approach to detect small leaks, changes in leak rates, crack movements, and movements or changes in the structure which may constitute a signal of the onset of increased hazards (a safety device). (d) Liquid Penetrant Inspection to detect surface cracking (primarily on convex deformations) that may be related to structural weakness. The technique is a secondary one on the initial approach to the tank car, but is easy to use and may potentially be most useful during the latter stages of the operation. Ultrasonic and acoustic emission sensing can be operated remotely from the same basic system, once the scanning devices and fixtures have been emplaced.

(3) NDE techniques potentially useful after unloading and during the recovery operations are: (a) Liquid Penetrant Inspection to detect surface-breaking defects on accessible surfaces. These are quicker and more precise, where applicable, than ultrasonics or radiography, and require less equipment. (b) Ultrasonics to detect buried flaws and defects and those breaking on inacessible surfaces. (c) Acoustic emission to detect and pinpoint structural responses to changes in loading stress and stress created as the car is unloaded or moved."

The BRL provided INEL with ten of the impacted plates discussed above for the purpose of performing a preliminary evaluation of NDE applications to tank car type steel to test our initial ideas concerning the general approach. The approach was to measure deformation parameters using NDE techniques and generate correlations with physical and metallurgical measurements of damage and residual structural strength. The rationale is that if reasonable correlations can be found, then remote observations may be used to establish probabilistic bounds on the structural integrity of the tank car. The bounds could be narrowed in successive states as personnel approach closer to the tank car since the shorter distances would allow them to make successively finer and more detailed measurements.

The NDE techniques used included visual inspection, liquid penetrant inspection, and various ultrasonic techniques. Figure 29 presents three views of one of the impacted plate specimens showing the general shape of the dent. Liquid penetrant inspections were done on both the convex and the concave sides of the ten plate specimens to determine the degree of surface cracking. A map was made for each specimen showing both size and location of all surface cracks and tears. A sample of such a map is presented in Figure 30. The sample shows no signs of cracking on the concave sides of the dent except for the tears when the thickness was completely penetrated. It was observed that the surface cracks run in the rolling direction of the steel which may be indicative that the manufacturing process influences the residual strength level.

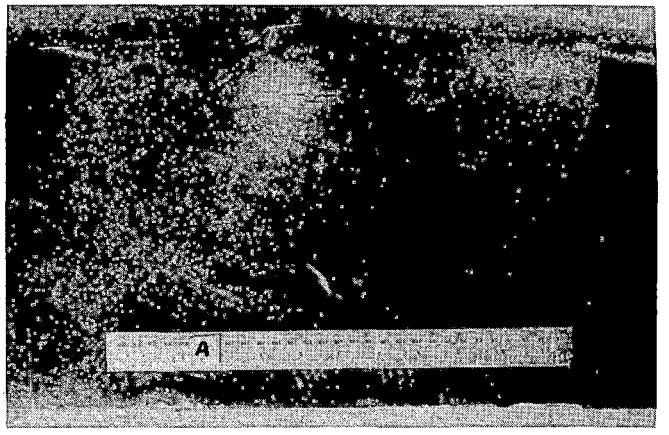


Figure 29 a: Convex (Bottom) Side of Flat Plate Specimen

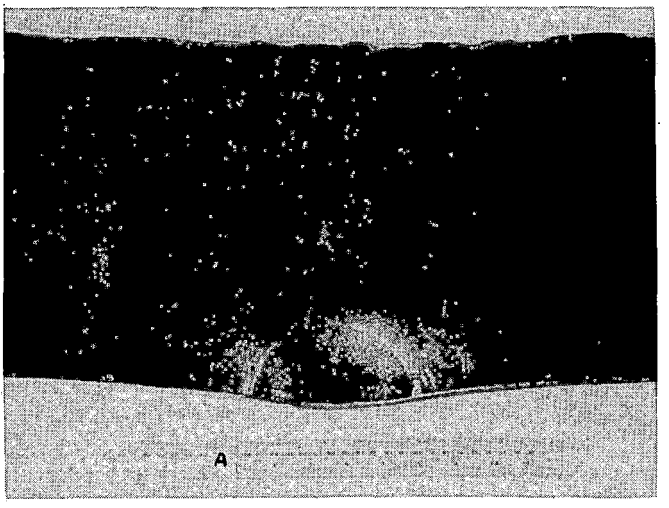


Figure 29 b: Impact Side of Flat Plate Specimen

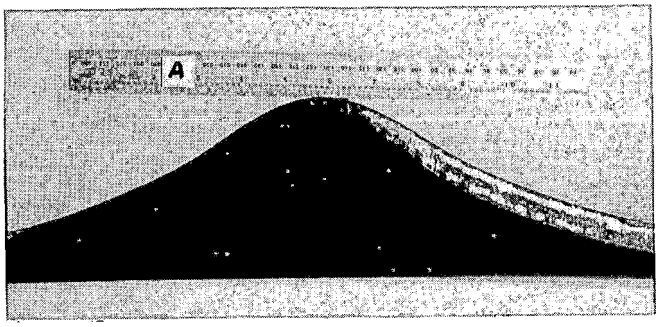


Figure 29 c: Cross-section of Flat Plate Specimen

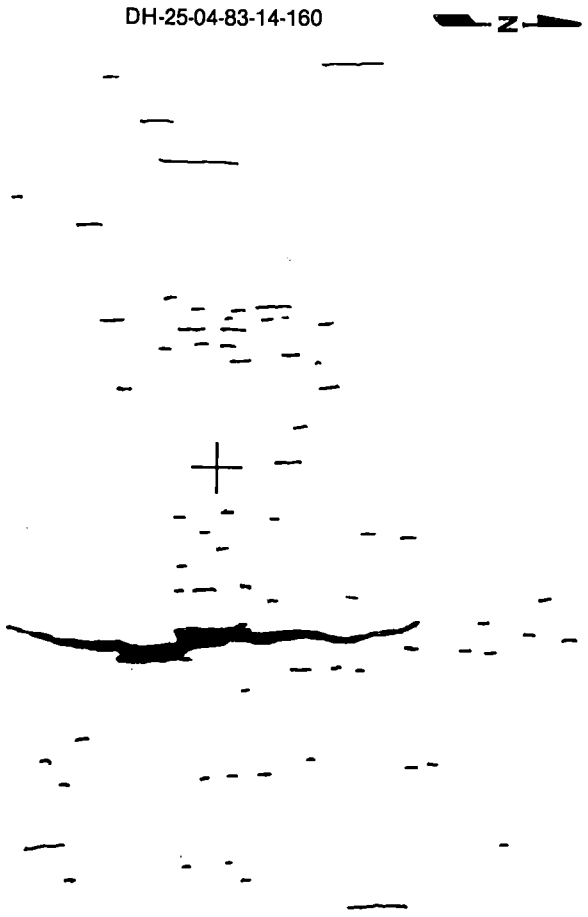


Figure 30: Surface Crack Map on Convex Side of Flat Plate Specimen

The thicknesses of the specimens were measured using an ultrasonic thickness gauge. Figure 31 presents an example of the plots showing the depth and radius of curvature of the dents and Figure 32 presents a typical plot of thickness as a function of position across the dent. It was found that easy visually observed fractures and tears were located in the areas of greatest thinning. Section thinning as much as 32% was observed. Figure 33 presents an example of typical areas of severe thinning which consist of two lobes on the thickness plot the plate specimen. Figure 34 presents a case where the thinning level was not severe. Those areas of greatest thinning constitute the points where the residual strength are in question.

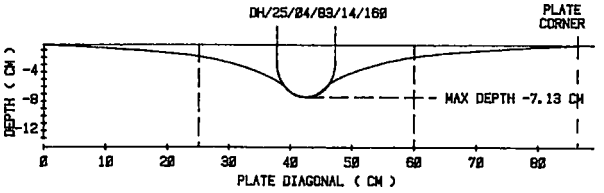


Figure 31: Dial Micrometer Measurements of Dent Depth

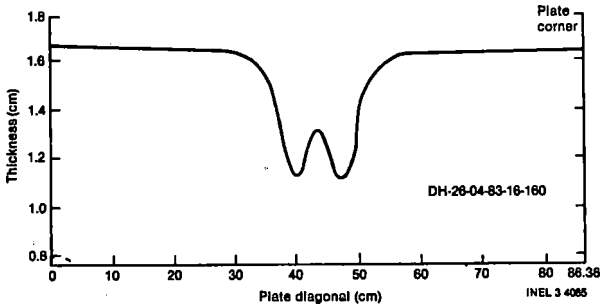


Figure 32: Typical Example of Thickness Versus Position for Flat Plate Specimens

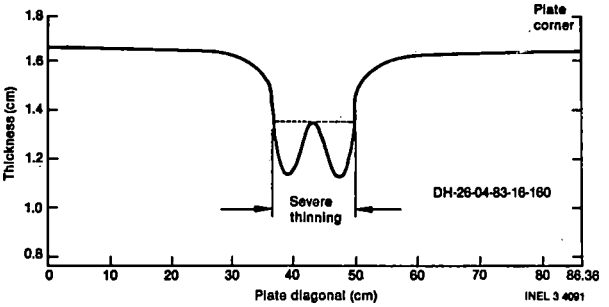


Figure 33: Thickness Plot Showing Severe Thinning

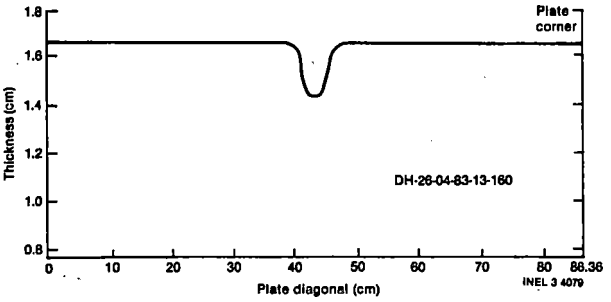


Figure 34: Thickness Plot Without Sufficient Deformation to Cause Severe Thinning

The total length of surface cracks, number of surface cracks, and the area size showing significant surface cracking compared with deformation are listed with their correlation coefficients in Table 5. Plots of area of surface cracking as a function of maximum depth of the dent, number of cracks as a function of maximum depth of dent, and the total length of cracks as a function of the maximum depth of dent are given in Figures 35 through 38. The correlations between some of these measurements are excellent and if these correlations are sustained statistically (with a much larger sample), then a valuable tool will be available for assessing the structural integrity of a damaged tank car from data which can be obtained from a remote and therefore safe location.

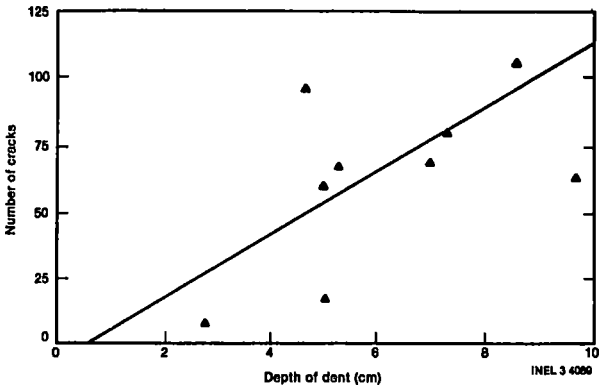


Figure 37: Number of Cracks Versus Dent Depth

TABLE 5: CORRELATION OF MEASURES OF DEGREE OF SURFACE CRACKING AND DEFORMATION

| Measure of Surface Cracking | Measure of Deformation | Y-Intercept | Slope | Correlation Coefficient |
|---|---|---|---|---|
| Total Length of Cracks | % Reduction in Thickness | -7.86 cm | 1.04 | 0.5409 |
| Area of Surface Cracking | % Reduction in Thickness | -49.33 $cm^2$ | 10.44 | 0.6921 |
| Total Length of Cracks | Dent Depth | -4.05 cm | 3.12 | 0.6875 |
| Number of Cracks | Dent Depth | -4.24 No. | 11.45 | 0.7039 |
| Area of Surface Cracking | Dent Depth | -8.66 $cm^2$ | 31.04 | 0.8698 |
| Total Length of Cracks | Radius of Curvature | -5.72 cm | 3.75 | 0.5486 |
| Number of Cracks | Radius of Curvature | -37.08 No. | 18.30 | 0.7472 |
| Area of Surface Cracking | Radius of Curvature | -90.59 $cm^2$ | 48.39 | 0.9010 |

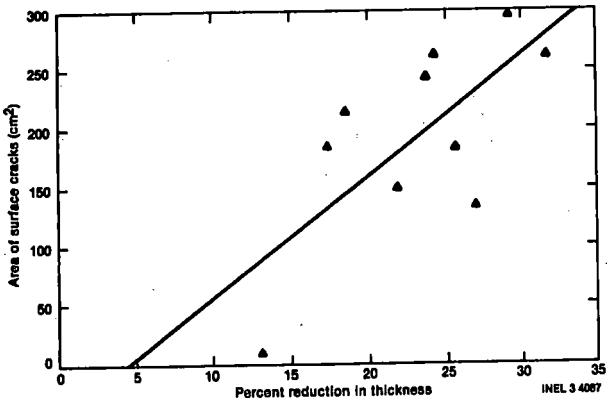


Figure 35: Area of Surface Cracking Versus Percent Reduction in Thickness

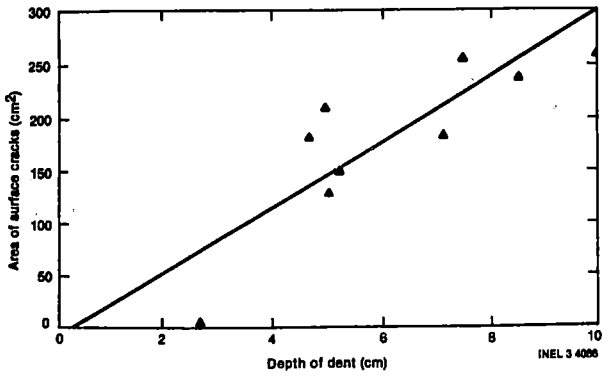


Figure 36: Area of Surface Cracking Versus Dent Depth

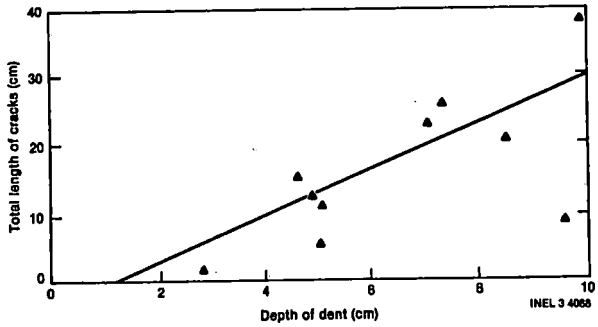


Figure 38: Total Length of Cracks Versus Dent Depth

The plates were examined using a computer-controlled ultrasonic imaging system for immersed ultrasonic testing. A photograph of the system used is presented in Figure 39. The areas in which it was assumed that information on distressed metal were (1) areas near known cracks, (2) areas in otherwise "sound" metal, (3) areas having relatively stronger echo signals at high frequencies than at low frequencies, and (4) areas having the same orientation as known cracks (which indicate stress directions). These properties were postulated for areas which contain severely disturbed metallurgy and therefore metal which may be on the verge of outright rupture.

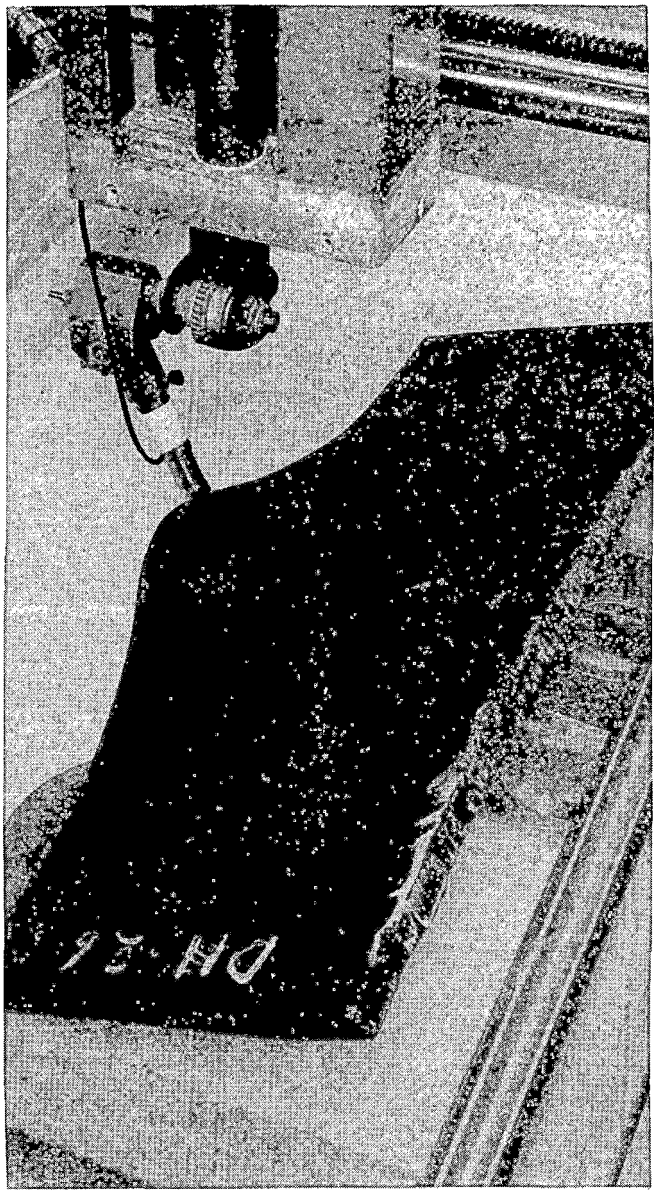

Figure 39: Ultrasonic Examination of Flat Plate Specimen

The ultrasonic measurements were made by scanning at a frequency of 2.25 MHz in conjunction with a computer-generated imaging for interpretation purposes. Figure 40 presents contour plots generated by this ultrasonic imaging system of flaws in the metal. The system produces maps of the area of interest in which the contours are lines of equal reflected sonic intensity. These maps are read much like one would a standard topographic map. The patterns made by the reflected sound are the "hills" of the topographic map, thus, giving a sonic picture of the flaw. The x-y plane is a top view of a small area of a plate specimen. The x-z and the y-z planes are two views of the thickness of the same area. Targets meeting the above postulated conditions were found in various areas evaluated in the plates. Small point-like targets, and some of slightly extended areas, were found in moderately deformed areas. Such targets were entirely absent in areas of little or no deformation, thus indicating that the targets in question are associated with deformation. If further work confirms current interpretation of the extended and point-like targets as representing severe and moderate damage preceding failure, respectively, and if the same or similar phenomena are found in other tank car materials, ultrasonic measurements made in situ on damaged tank cars will be a powerful tool for assessing tank car status in the field.

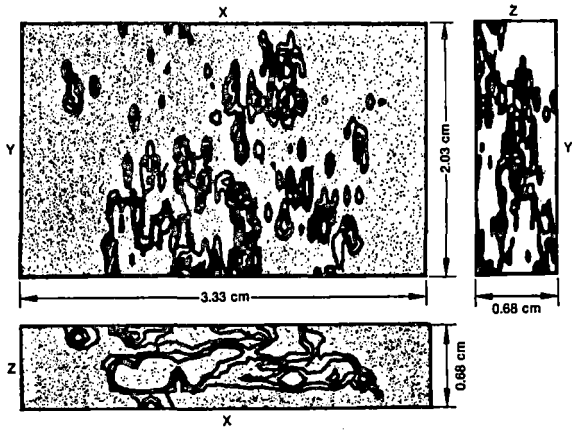


Figure 40: Flaw Contour Plots Generated by an Ultrasonic Imaging System

Once the flaws are identified and described in the damaged tank car, the seriousness of the flaws in terms of potential rupture must be determined in accordance with a data base consisting of probability of rupture as a function of applied stress. In order to obtain this basic data, a parallel study in fracture mechanical evaluation of damaged material is essential. Tank car failure occur due to an interaction of applied stress and defects (cracks) and this can be quantified using linear-elastic fracture mechanics (LEFM).

For the purpose of demonstration of the methodology and to yield useful data for the problem at hand, several of the impacted steel plates were studied by fracture mechanics. A literature search was made for basic characteristic data for ASTM A515, Grade 70 type steel. Of special interest was the parameter Plane Strain Fracture Toughness ($K_{Ic}$) because when the Applied Stress Intensity Factor ($K_I$) equals the former, failure (rupture) occurs.

Two plates were analyzed for estimating the fracture toughness of the undeformed and the deformed material. Figures 41 and 42 presents schematics of the two plates showing the thickness measurements and the location of test specimens. Time and material limitations prevented the development of valid Plane Strain Fracture Toughness ($K_{Ic}$) measurements. Thus estimates were made using the True Stress-True Strain curve developed from tensile specimens and these are listed in Table 6. These tests were conducted at 294 $^{o}$K (70 $^{o}$F).

Since surface flaws of the same size as embedded flaws are more detrimental, assuming each is exposed to similar stresses, the follow-

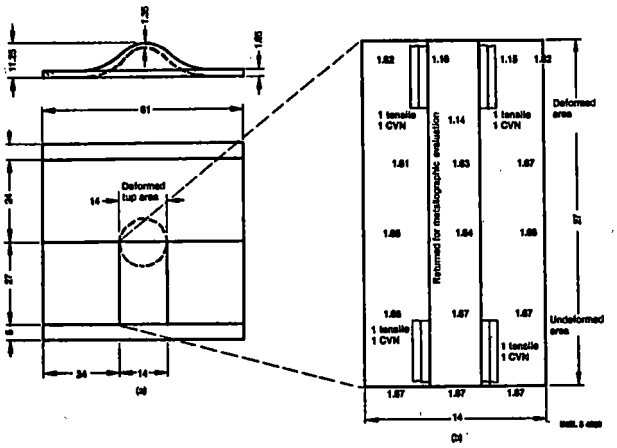

Figure 41: Thickness Measurements (mm) and Locations of Test Specimens Removed From Plate DH-2B-04-83-160; a. General Schematic, b. Section Removed From Plate

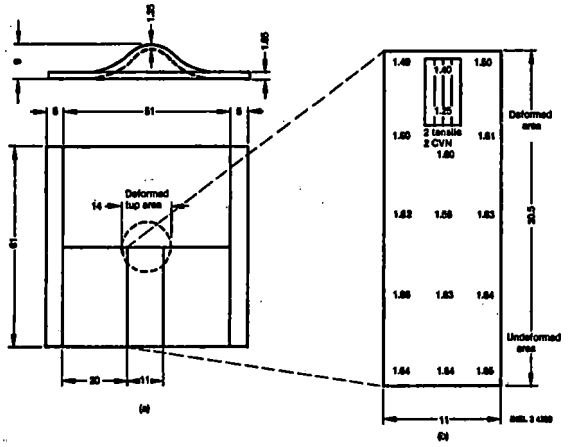

Figure 42: Thickness Measurements (mm) and Locations of Test Specimens Removed From Plate DH-2B-04-83-22-160; a. General Schematic, b. Section Removed From Plate

ing deals with surface flaws for demonstration purposes. The two analyses are for an undamaged tank car where the critical flaw size is calculated based on an applied stress of 161 MPa (22.3 ksi) and $K_{Ic}$ of 110 MPa * $m^{1/2}$ (100 ksi * $in.^{1/2}$) presented in Table 6 and for a damaged tank car where the maximum allowable stress is calculated using $K_{Ic}$ = 44 MPa * $m^{1/2}$ (40 ksi * $in.^{1/2}$) and the crack depth corresponding to those measured by NDE. The correlation between applied stress and flaw sizes is given in Figure 43. This figure can be used to determine the critical crack depth for a given value of $K_{Ic}$. Values of $K_{Ic}$ for damaged tank cars of wall thickness of 12.2 mm (0.48 in.) are presented in Figure 44. Since the data base of fracture toughness parameters versus temperature is inadequate for developing a statistically based correlation between $K_{Ic}$ and temperature, it was necessary to estimate $K_{Ic}$ to illustrate the analytical approach for calculating the critical flaw depth, for undamaged tank cars, and for calculating the critical flaw depth-stress correlation for damaged tank cars.

For undamaged tank cars, the estimate of $K_{Ic}$ = 110 MPa * $m^{1/2}$ (100 ksi * $in.^{1/2}$) in Table 6 for material at 294 °K (70 °F) was used to calculate the critical crack depth (i.e., that which would cause failure) if the 16.3 mm (0.64 in.) thick wall was exposed to a stress of 161 MPa (23.3 ksi). The results of these calculations are shown in Figure 43 for two aspect ratios, a/2c = 0.1 and a/2c = 0.5, where 2c is crack length and "a" is the crack depth. The peak $K_I$ values occur at maximum depth for a/2c = 0.1 and at the free surface for a/2c = 0.5. Experimental evidence suggests that when $K_I$ (at the free surface) = $K_{Ic}$ crack initiation will frequently not occur due to the plane stress (as opposed to plain strain) condition at the free surface. Under plane stress conditions $K_{critical}$ is greater than $K_{Ic}$; therefore, crack initiation occurs somewhere else around the perimeter of the crack. The curves represented by the solid triangles and the open circles in Figure 43 bound the conditions for failure. For analytical purposes, a conservative estimate was made that the failure conditions are governed by the plot for a/2c = 0.1 in Figure 43. The calculated conditions for failure are given in Table 7.

TABLE 6: MECHANICAL PROPERTIES FOR PLATES 16 AND 22

| Specimen Identification | Thickness (cm) | Thickness (in.) | Yield Strength (MPa) | Yield Strength (ksi) | Ultimate Strength (MPa) | Ultimate Strength (Ksi) | Cold Work (%) | Estimated $K_{Ic}$ (MPa*$M^{1/2}$) | Estimated $K_{Ic}$ (ksi*$in.^{1/2}$) |
|---|---|---|---|---|---|---|---|---|---|
| 16-3 | 1.651 | 0.650 | 338 | 49 | 538 | 78 | 0 | 128 | 116 |
| 16-2 | 1.575 | 0.620 | 476 | 69 | 593 | 86 | 4.5 | 117 | 106 |
| 16-1 | 1.567 | 0.617 | 490 | 71 | 593 | 86 | 5.1 | 111 | 101 |
| 16-4 | 1.130 | 0.445 | 765 | 111 | 800 | 116 | 31.5 | 48 | 44 |
| 22-3 | 1.626 | 0.640 | 317 | 46 | 558 | 81 | 1.5 | 111 | 101 |
| 22-1 | 1.575 | 0.620 | 469 | 68 | 600 | 87 | 4.6 | 112 | 102 |
| 22-2 | 1.562 | 0.615 | 483 | 70 | 600 | 87 | 5.4 | 90 | 82 |
| 22-4 | 1.232 | 0.485 | 710 | 103 | 772 | 112 | 25.4 | 46 | 42 |

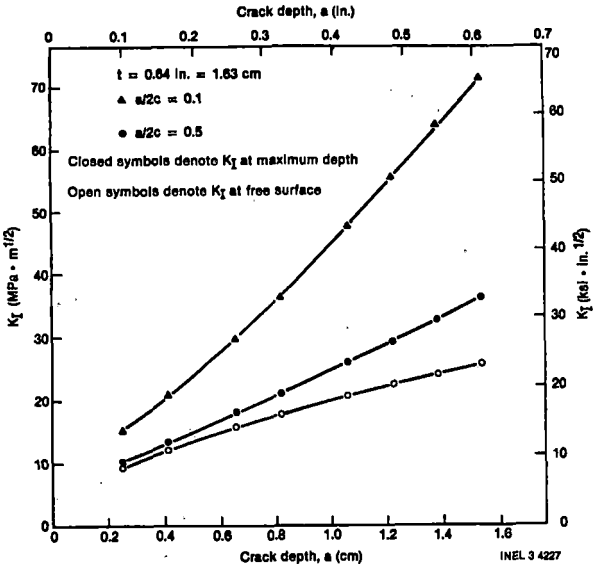


Figure 43: Applied Stress Intensity Factor and Crack Depth for Undamaged Tank Car

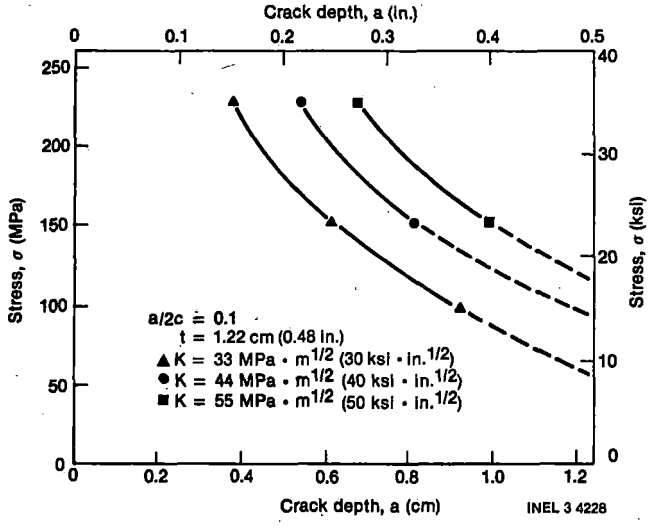


Figure 44: Applied Stress and Crack Depth With a/2c = 0.1

For the damaged tank cars where the wall thickness has been reduced 25%, Table 6 shows the estimated value of $K_{Ic}$ = m½ (40 ksi * in.½). Figure 44 shows a plot of critical stress versus crack depth for three values of $K_{Ic}$. An example of how these plots may be used is as follows: (1) NDE revealed an estimated average crack length of 1.27 cm (0.5 in.) (disregarding the small defects) and a maximum crack length of 44.5 mm (1.75 in.) ( not penetrating the wall thickness). These measurements were obtained from plates 16 and 22 where 349.3 mm (13.75 in.) and 279 mm (11.0 in.) die diameters were used, respectively, with a 140 mm (5.5 in.) tup, and (2) $K_{Ic}$ = 44 MPa * m½ (40 ksi * in.½). (3) Figure 44 shows for a/2c = 0.1, if a = 0.44 cm (0.175 in.), then the critical stress is approximately 102 MPa (40 ksi).

A similar set of curves for a/2c = 0.5, presented in Figure 45, are used to make a comparison of the critical stresses shown in Table 7. For $K_{Ic}$ = 44 MPa * m½ (40 ksi * in.½): (1) If 2c = 12.7mm (0.5 in.) and a = 6.4 mm (0.25 in.), then the critical stress is equal to 372 MPa (54 ksi) which appears to be less than the extrapolated value in Figure 44 for a/2c = 0.1 for the same crack length. (2) If 2c = 23.4 mm (0.92 in.) and a = 11.7 mm (0.46 in.), then the critical stress is equal to 223 MPa (32.3 ksi). For $K_{Ic}$ = 33 MPa * m½ (30 ksi * in.½): (1) If 2c = 23.4 mm (0.92 in.) and a = 11.7 mm (0.46 in.), then the critical stress is equal to 60.5 MPa (23.8 ksi).

These calculations illustrate the potential applicability of LEFM techniques for predicting failure conditions, e.g., structural integrity of damaged tank cars. The next requirement is to relate the change in $K_{Ic}$ as a function of deformation, which requires information regarding the magnitude of deformation for actual damaged tank cars. It would then be necessary to develop a correlation between reduction in thickness and change in $K_{Ic}$. The sensitivity of the critical crack depth to stress shown in Figure 44 indicates that a stress analysis of typical damaged tank cars using different loading points and techniques during movement is needed. The magnitude of these calculated stresses could be used

TABLE 7: CALCULATED CONDITIONS FOR FRACTURE*

| Tank Car Condition | $K_{Ic}$ (MPa * m$^{1/2}$) | $K_{Ic}$ (ksi * in.$^{1/2}$) | Critical Stress (MPa) | Critical Stress (ksi) | Flaw Depth (a) for a/2c = 0.1 (mm) | Flaw Depth (a) for a/2c = 0.1 (in.) | Flaw Depth (a) for a/2c = 0.5 (mm) | Flaw Depth (a) for a/2c = 0.5 (in.) |
|---|---|---|---|---|---|---|---|---|
| Undamaged | 110 | 100 | 160.8 | 23.3 | 16.3 | 0.64 | — | — |
| | 44 | 40 | 160.8 | 23.3 | 9.9 | 0.39 | — | — |
| Damaged | 44 | 40 | 241.5 | 35.0 | 1.3 | 0.05 | — | — |
| | 44 | 40 | 276.0 | 40.0 | 4.4 | 0.18 | — | — |
| | 33 | 30 | 276.0 | 40.0 | 1.3 | 0.05 | — | — |
| | 33 | 30 | 276.0 | 31.3 | 4.4 | 0.18 | — | — |
| | 44 | 40 | 372.6 | 54.0 | — | — | 6.4 | 0.25 |
| | 44 | 40 | 222.9 | 32.3 | — | — | 11.7 | 0.46 |
| | 33 | 30 | 276.0 | 40.0 | — | — | 6.4 | 0.25 |
| | 33 | 30 | 164.2 | 23.8 | — | — | 11.7 | 0.46 |

*If crack depth (a) is defined, then the calculated stress is the critical stress; but if stress is given, then the calculated crack depth is a critical value.*

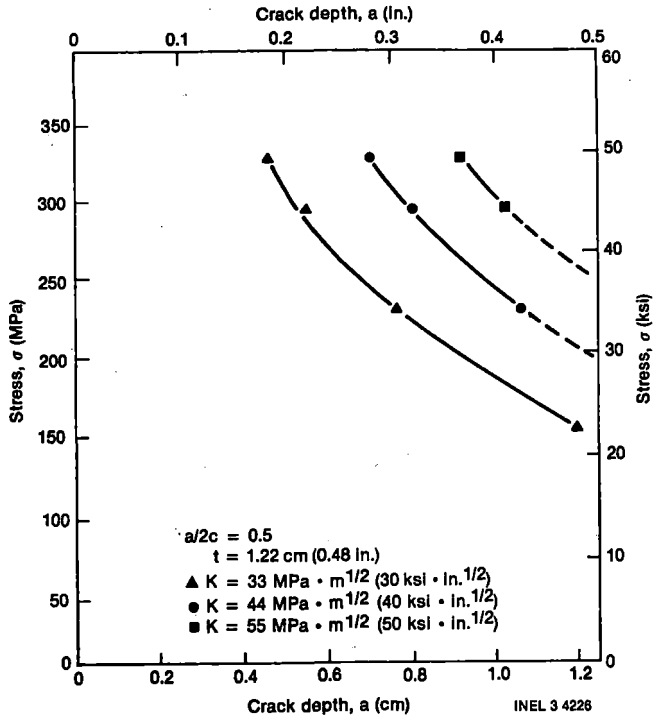


Figure 45: Applied Stress and Crack Depth With a/2c = 0.5

in conjunction with the data in Figure 44 to estimate the accuracy needed for measurements of $K_{Ic}$ and NDE measurements of crack depth. No discussion of weldments has been attempted in the study thus far, but these are potentially the most vulnerable areas from the viewpoint of a failure.

This study was undertaken as a reconnaissance effort and was limited in time and scope. The objectives were to attempt to define more clearly the scope of the overall problem and the areas in which future NDE and fracture mechanics/metallurgical efforts might profitably be directed. The experimental NDE effort provided very encouraging results, in nearly every instance confirming initial hypotheses on what could be expected. The results show that there are a number of field-observable NDE quantities (beyond the obvious ones of surface-breaking cracks) which seem to correlate with important mechanical parameters. The critical values of applied stress-crack size calculated for different values of $K_{Ic}$ show the usefulness of the fracture mechanics concepts and identify areas where additional work needs to be performed. Based on a fracture mechanics analysis, each of the parameters required for predicting the safety of moving a damaged tank car has been identified, and recommendations to increase accuracy while reducing conservatism has been provided. The decisions concerning which base material and types of weldments which should be studied in future work should be based on relative use of the materials in fabricating railroad tank cars.

## RECOMMENDATIONS

The work performed to date indicates that the best approach is to develop a data base consisting of (1) types of flaws existing in damaged tank car materials due to impacts, (2) failure levels as functions of applied stress for each type of flaw, and (3) to predict the applied stress due to movement of the tank car or the unloading of the tank car's lading. Once correlations are determined between these various sets of data, a series of methods using NDE equipment to determine the number, type, and location of flaws in the damaged tank car will permit an accurate prediction of possible failure. The effort thus far indicates favorably that such a goal is possible.

Follow-on tasks which are recommeded are: (1) A data base consisting of categories of flaws in tank car materials should be developed. The flaws can be created by drop hammer impacts on flat plates or models or perhaps actual damaged tank cars are available. (2) A study of the basic data should be conducted to determine correlations between flaw characteristics, observables, and metalurgical (fracture mechanics) parameters with further correlations with levels of applied stress leading to failure. (3) An elastic-plastic stress analysis of typical damaged tank cars is needed to determine the levels of stress expected during tank car wreck clearance operations. (4) Model tank cars should be tested using developed technology, and, after appropriate adjustments in the technology, a full scale tank car test should be conducted for final verification.

## REFERENCES


1. "Railroad Accident Report-Derailment of Louisville and Nashville Railroad Company's Train No. 584 and Subsequent Rupture of Tank Car Containing Liquefied Petroleum Gas, Waverly, Tennessee, February 22, 1978", NTSB-RAR-79-1, U.S. National Transportation Safety Board, Washington, D.C. 20594, 8 February, 1979.

2. "Railroad Accident Report-Louisville and Nashville Railroad Company Freight Train Derailment and Puncture of Hazardous Materials Tank Cars, Crestview, Florida, April 8, 1979", NTSB-RAR-79-11, U.S. National Transportation Safety Board, Washington, D.C. 20594, September 1979.

3. "SPECIAL INVESTIGATION REPORT — Tank Car Structural Integrity After Derailment", NTSB-SIR-80-1, U.S. National Transportation Safety Board, Washington, D.C. 20594, October 16, 1980.

4. Beissner, R.E., "Electromagnetic-Acoustic Transducers, A Survey of the State-Of-The-Art", Southwest Research Institute, San Antonio, Texas, NTIAC-76-1, January 1976.

5. Silvus, Jr., H.S., "Advanced Ultrasonic Testing Systems, A State-Of-The-Art Survey", Southwest Research Institute, San Antonio, Texas, NTIAC-77-1, September 1976

[6]Beissner, R.E., en tal, "NDE Applications of Magnetic Leakage Field Methods, A State-Of-The-Art Survey", NTIAC-80-1, January 1980, Southwest Research Institute, San Antonio, Texas 78284

[7]Matzkanin, G.A., en tal, "The Barkhausen Effect and Its Applications to Nondestructive Evaluations", NTIAC-79-2, October 1979, Southwest Research Institute, San Antonio, Texas 78284

[8]Gardner, G.C., "Automated Radiography - A State-Of-The-Art Survey", NTIAC-78-1, June 1978, Southwest Research Institute, San Antonio, Texas 78284

[9]Ash, J. Ivan, "Liquid Crystals For Nondestructive Evaluation", NTIAC-78-2, September 1978, Southwest Research Institute, San Antonio, Texas, 78284

[10]Yocum, Russell, "NDT of Damaged 1/5 Scale Railroad Tank Car", Report No. 83-N-4, June 29, 1983, Materiel Testing Directorate, Aberdeen Proving Ground, Maryland 21005

[11]Beller, L.S., en tal, "Survey of Nondestructive Methods for Evaluating Derailed Tank Cars," BRL Contract Report to be published, Ballistic Research Laboratory, Aberdeen Proving Ground, Maryland 21005